



# A Sedimentological Process-Based Approach To Depositional Reservoir Quality of Deep-Marine Sandstones

DOI:  
[10.2110/jsr.2016.74](https://doi.org/10.2110/jsr.2016.74)

**Document Version**  
Final published version

[Link to publication record in Manchester Research Explorer](#)

## **Citation for published version (APA):**

Porten, K. W., Kane, I., Warchol, M. J., & Southern, S. J. (2016). A Sedimentological Process-Based Approach To Depositional Reservoir Quality of Deep-Marine Sandstones: An Example From the Springar Formation, Northwestern Vøring Basin, Norwegian Sea. *Journal of Sedimentary Research*. <https://doi.org/10.2110/jsr.2016.74>

**Published in:**  
Journal of Sedimentary Research

## **Citing this paper**

Please note that where the full-text provided on Manchester Research Explorer is the Author Accepted Manuscript or Proof version this may differ from the final Published version. If citing, it is advised that you check and use the publisher's definitive version.

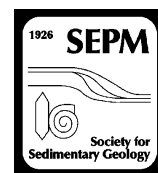
## **General rights**

Copyright and moral rights for the publications made accessible in the Research Explorer are retained by the authors and/or other copyright owners and it is a condition of accessing publications that users recognise and abide by the legal requirements associated with these rights.

## **Takedown policy**

If you believe that this document breaches copyright please refer to the University of Manchester's Takedown Procedures [<http://man.ac.uk/04Y6Bo>] or contact [uml.scholarlycommunications@manchester.ac.uk](mailto:uml.scholarlycommunications@manchester.ac.uk) providing relevant details, so we can investigate your claim.





## A SEDIMENTOLOGICAL PROCESS-BASED APPROACH TO DEPOSITIONAL RESERVOIR QUALITY OF DEEP-MARINE SANDSTONES: AN EXAMPLE FROM THE SPRINGAR FORMATION, NORTHWESTERN VØRING BASIN, NORWEGIAN SEA

KRISTIN W. PORTEN,<sup>1</sup> IAN A. KANE,\*<sup>1</sup> MICHAŁ J. WARCHOŁ,<sup>1</sup> AND SARAH J. SOUTHERN<sup>2</sup>

<sup>1</sup>Statoil ASA, N-5020 Bergen, Norway

<sup>2</sup>School of Earth and Environment, University of Leeds, U.K.

e-mail: KRISP@statoil.com

**ABSTRACT:** Reservoir properties of deep-marine sandstones deposited by various sediment-gravity-flow types in the northwestern Vøring Basin (Norwegian Sea) are characterized using detailed sedimentological and petrographic analyses. The sandstones are quartz arenites and subarkoses, having similar mineralogical compositions, a low degree of diagenetic modification, and low to moderate volumes of quartz cement (up to 6%). However, significant textural variability is observed for the various sandstone types, which were subdivided based upon their interpreted processes of deposition. In the studied wells there is a predominance of turbidites deposited by high-density turbidity currents (HDTs) and a range of hybrid event beds (HEBs). HDTs are coarser grained and contain less detrital clay than the various HEBs. In addition, the dominant grain size of HEBs decreases down the depositional profile whilst the content of detrital clay increases. Porosities of the various bed types span the same interval, but overall the HDTs and proximal HEBs have a higher proportion of samples with porosities higher than 20%, compared to distal HEBs. Permeabilities, in contrast, are significantly different, with the HDTs having permeabilities approximately two orders of magnitude higher than clay-rich HEBs. A comparison of the observed variability in composition and textural parameters with porosity and permeability indicates that sedimentological flow processes control the depositional reservoir quality of deep-marine sandstones; understanding these processes therefore enhances our ability to predict distribution of reservoir quality in deep-marine systems.

### INTRODUCTION

Porosity and permeability are controlled by the types of grains, matrix, and pore systems making up a reservoir rock (e.g., Ehrenberg 1990; Wilson and Stanton 1994; Ramm 2000; Taylor et al. 2010; Walderhaug et al. 2012), and only through combined petrological and sedimentological studies can we attempt to predict evolution of reservoir quality from deposition through burial (Bloch and McGowen 1994; Morad et al. 2010; Bjørlykke 2014). Petrological studies are key to our understanding of the factors controlling porosity and permeability, from original sediment composition and texture to sediment modification and lithification during burial in response to mechanical compaction and diagenetic processes (e.g., Bloch 1994; Wilson and Stanton 1994; Morad et al. 2010; Bjørlykke 2014). Sedimentological investigations are essential in order to predict original sediment composition and texture, facies distribution, and sand-body geometry (e.g., Pirmez et al. 2000; Hodgson et al. 2006; Kane and Pontén 2012). As recently pointed out by Bjørlykke (2014), there is a tendency for petrological and sedimentological studies to be carried out as two separate disciplines, while close integration of all available geological information is needed to better constrain reservoir quality prediction and reservoir understanding. “Depositional sand quality” is defined by Ehrenberg (1997) as the combined effect of

primary sand composition and texture, and early diagenetic processes imparted by the depositional environment upon reservoir quality. Determining depositional sand quality in turn provides a tool for predicting porosity and permeability in response to sediment burial and diagenetic alterations.

Experimental studies of artificially mixed and packed clay-free unconsolidated sands show that original porosity and permeability are determined mainly by grain size, sorting, and packing of grains (Fraser 1935; Beard and Weyl 1973). In sands containing more than a few percent of clay, permeability will, in addition, be strongly controlled by clay volume and distribution (Fraser 1935). These primary properties are controlled by sediment source area, transport history—including effects of the receiving-basin geometry and seafloor composition, depositional processes, and early postdepositional modification by, e.g., bioturbation and precipitation of early cements. Studies of recent sands from various shallow-marine and terrestrial environments confirm the textural control on sediment porosity and permeability (Pryor 1973), and reservoir quality of deep-marine sandstones of various ages and basins has been shown to vary significantly due to differences in original sediment composition and texture (Marzano 1988; Lien et al. 2006; Ehrenberg et al. 2008; Njoku and Pirmez 2011; Kilhams et al. 2012; Marchand et al. 2015). However, the general inaccessibility of modern deep-marine systems renders them one of the least-well understood sedimentary environments, and hence predicting reservoir quality of deep-marine systems both pre- and postdrill is a

\* Present Address: School of Earth, Atmospheric and Environmental Sciences, University of Manchester, U.K.

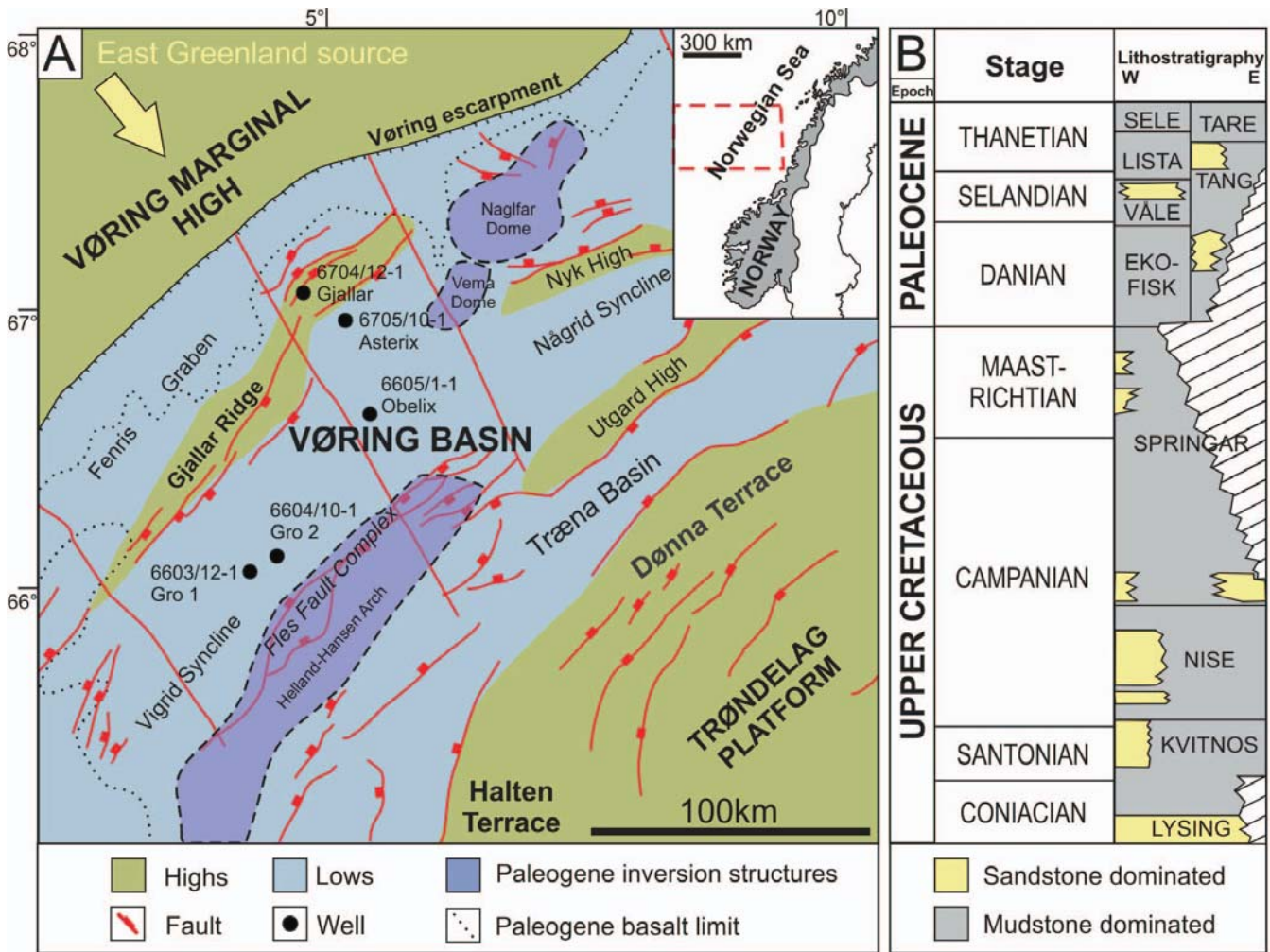


FIG. 1.—A) Location of study area with well locations, and B) simplified stratigraphy of the Vøring Basin (figure modified from Brekke et al. 1999; Færseth and Lien 2002; Fjellanger et al. 2005).

significant challenge to the hydrocarbon industry. With the exception of the work by Lien et al. (2006), Njoku and Pirmez (2011), Kilhams et al. (2012), and Marchand et al. (2015), little (published) systematic research has examined the relationship between sedimentary facies and reservoir quality of deep-marine sandstones, in order to enhance prediction of reservoir quality in deep-marine fan systems. Here we attempt to bridge this gap by investigating the relationship between depositional sand quality and reservoir properties of deep-marine sandstones deposited by various sediment-gravity-flow types in a Maastrichtian submarine-fan system located in the Gjallar Ridge–Vigrid Syncline area in the northwestern part of the Vøring Basin (Norwegian Sea, Norwegian continental shelf). The term “depositional reservoir quality” is introduced to describe the initial reservoir potential imparted on the deposits of discrete flow types prior to postdepositional modification. Using a combined petrological and sedimentological approach we address the following key questions: 1) What is the nature of depositional reservoir quality across the range of various deep-marine sediment-gravity-flow deposits? 2) Do specific sedimentological processes create deposits with characteristic depositional reservoir quality? 3) Is the process bed-type approach a useful step towards predictability of reservoir-quality distribution in deep-marine sediment-gravity-flow systems?

GEOLOGICAL SETTING

The Vøring Basin is located 300 km west of mid-Norway in the Norwegian Sea on the Norwegian continental shelf (Fig. 1A). The basin developed during two regionally extensive rifting episodes of Late Jurassic to Early Cretaceous and Late Cretaceous to Paleocene age that culminated in the opening of the Atlantic Ocean (Skogseid and Eldholm 1989; Roberts et al. 1997; Færseth and Lien 2002). The Lysing, Kvitnos, Nise, and Springar formations are deep-marine sedimentary units which form the upper Cretaceous stratigraphy in the Vøring Basin (Fig. 1B). Whilst the Lysing Formation was generally deposited on broad regional basin slopes, such as those of the Halten and Dønna Terraces and the Agat area (Martinsen et al. 2005), the Kvitnos, Nise, and Springar formations were influenced by local basin topography associated with the early stage of the Late Cretaceous–Paleocene rifting (Færseth and Lien 2002; Lien et al. 2006).

The Springar Formation of this study is mudstone-dominated, but with thick sandstone packages originating from deposition within submarine-fan systems infilling local basin-floor topography (Lien et al. 2006). The gravity-flow deposits are dominated by fine-grained and clay-rich sandstones of Campanian to Maastrichtian age (Færseth and Lien 2002; Lien et al. 2006, Southern et al. in press), sourced from the uplifting East



TABLE 1.—Sample material Springar Formation, wells 6704/12-1 (Gjallar), 6705/10-1 (Asterix), 6605/1-1 (Obelix), 6603/12-1 (Gro 1), and 6604/10-1 (Gro 2).

Well name	Well no.	Formation	Point-counted thin sections	Core-plug measurements	Material	Cored interval, mRKB	Thickness cored interval, m
Gro 1	6603/12-1	Springar	16	82	Core	3714.00–3732.47	18.47
Gro 2	6604/10-1	Springar	24	232	Core	3601.40–3655.27	53.87
Obelix	6605/1-1	Springar	16	103	Core	3239.00–3266.10	27.10
Gjallar	6704/12-1	Springar	7	69	Core	2559.00–2574.70 2997.00–3005.40	24.10
Asterix	6705/10-1	Springar	19	423	Core	3226.00–3327.30	101.30
<b>Total:</b>	<b>5</b>		<b>82</b>	<b>909</b>			<b>224.84</b>

Greenland margin (Fonneland et al. 2004; Morton et al. 2005; Slama et al. 2011). In this study the Springar Formation has been investigated in five exploration wells located along an approximately down-dip depositional transect (Gjallar–Gro transect) in the Gjallar Ridge–Vigrig Syncline area (Fig. 1A).

#### SAMPLE MATERIAL AND METHODS

To assess the link between depositional facies and reservoir quality, detailed thin-section studies and porosity and permeability plug measurements of core samples were combined with sedimentological interpretation of the sampled facies. The available sample material comprises 82 thin sections and 909 core plug measurements of porosity and permeability from 225 m of core from the Springar interval in exploration wells 6704/12-1 (Gjallar), 6705/10-1 (Asterix), 6605/1-1 (Obelix), 6603/12-1 (Gro 1), and 6604/10-1 (Gro 2) (Table 1). Although bioturbation on the whole is minor, samples were selected from undisturbed areas to avoid the potential for postdepositional disturbance of original sediment texture. Thin sections were mostly made from plug trimmings from the plugs used for routine measurements of helium porosity and permeability, and partly from core chips (Gro wells; 6603/12-1 and 6604/10-1). All thin sections were examined with a petrographic microscope, and point-counted with 300 points per thin section (Appendix, see Supplemental Material). Grain size was determined for all samples by measuring the long axes of 150 point-counts of silt and sand grains and then calculating the average value for each sample (Appendix). Sorting was defined as the sample standard deviation of the 150 grain-size measurements divided by the mean grain size (= coefficient of variation, Appendix).

In addition, a selection of samples was studied and photographed using a scanning electron microscope (Hitachi S-3400N SEM) for clay-mineral element composition, morphology, and distribution.

The permeabilities discussed in the text and presented on figures are Klinkenberg-corrected horizontal gas permeabilities from routine core analysis.

#### RESULTS

##### Bed Types

A process-based bed-type classification scheme was used to subdivide the studied core intervals (Figs. 2, 3). Each of these bed types is linked to a specific flow process, or range of processes, which has implications for the interpretation of the depositional environment and therefore the spatial distribution of facies and reservoir quality. This approach is favored over a purely lithofacies-based approach, as, in conjunction with geomorphological data, a degree of predictability is achieved which may be useful for reservoir modeling and paleoenvironmental interpretation.

The studied deep-marine system is dominated by fine-grained and clay-rich sandstones (Figs. 3, 4), interpreted here as hybrid event beds (HEBs, Haughton et al. 2003; Haughton et al. 2009; Talling et al. 2012). The HEBs

are subdivided into proximal and distal types due to their distribution along the inferred depositional transect (see Fig. 2 for description). Proximal HEB types usually have a relatively clean and unstratified division at their bases, grade upwards into argillaceous and micaceous color-banded sandstones with common dewatering structures, and are occasionally capped by a chaotic and muddy division with rip-up clasts. The color-banded sandstones are the dominant facies of this bed type, and the proximal HEBs are broadly equivalent to “slurry beds” of Lowe and Guy (2000), HEBs dominated by color-banded sandstone facies described by Barker et al. (2008), Davies et al. (2009), and Haughton et al. (2009), and transitional-flow deposit types I–III of Kane and Pontén (2012). The distal HEB types typically have tens-of-centimeters-thick planar-parallel-stratified divisions at their bases, grade upwards into a color-banded division with scattered dewatering features, and are capped by a thick (up to about 1 m) chaotic and muddy division with common rip-up clasts (Fig. 5). The color-banded division in distal HEBs is typically thinner than in the proximal HEBs, and the unstratified division at bed bases is thinner or absent. These deposits are similar to some of the HEBs described by Haughton et al. (2009), and to transitional-flow deposit types IV–VI of Kane and Pontén (2012).

Unstratified fine- to medium-grained and clay-poor sandstones have been interpreted as high-density turbidites (HDTs; the term used here for turbidites deposited from high-density turbidity currents, *sensu* Lowe 1982, Fig. 4A). Thin-bedded and entirely laminated silty to very fine-grained low-density turbidites (LDTs; the term used here for turbidites deposited from low-density turbidity currents, *sensu* Lowe 1982), thin- to medium-bedded mud-rich debrites (D), thin-bedded very fine- to fine-grained bottom-current-reworked sandstones (BCRS), and thin- to medium-bedded very fine- to coarse-grained weakly stratified tractional lag deposits (TLD) are present but are volumetrically less important in the studied part of the Gjallar–Gro transect, than HDTs and HEBs (Figs. 3, 4).

##### Bed-Type Distribution

A general downslope transition is observed from dominantly HDTs in the most proximal area (Gjallar), to a proximal HEB-dominated section with subordinate HDTs, slumps, and debrites (Asterix and Obelix), and to a distal HEB-dominated section with lesser proximal HEBs and LDTs in distal areas (Gro wells) (Figs. 1, 3). It is not straightforward to link the bed types to a downslope evolution of flows, as the event beds intersect different parts of the Springar Formation stratigraphy and cannot be correlated between wells. Nevertheless, in the studied HEBs there is a strong downslope trend of decreasing grain size and increasing clay content.

The most proximal well, Gjallar, is dominated by HDTs in the upper stratigraphic interval, and contains a section dominated by distal HEBs and local debrites in the lower stratigraphic interval. Asterix, the next well down depositional dip, is dominated by thick packages of amalgamated proximal HEBs, and lesser debrites and slumps. In its upper part there are


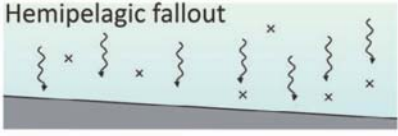
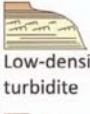


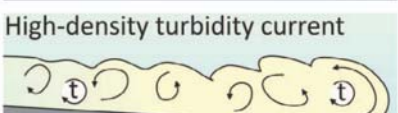
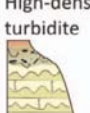
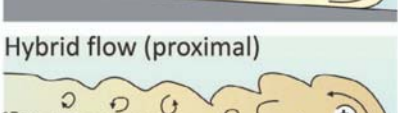
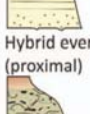


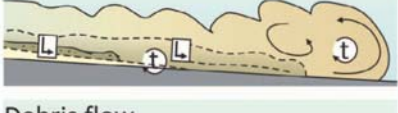
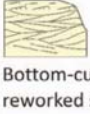



	Bed type	Process / flow type	Bed type description	Interpretation
Background	 Hemipelagite	 Hemipelagic fallout	Bed thickness: few mm to 5 m. Grain size: clay, minor silt. Sedimentary structures: structureless or laminated (facies Mm).	Suspension fallout from water column.
Sediment gravity flow deposits	 Low-density turbidite	 Low-density turbidity current	Bed thickness: few cm to 30 cm. Grain size: si-vf. Sedimentary structures: plane-parallel and ripple cross lamination throughout (facies Ss), normally graded.	Competence-related deposition and tractional working by low-density turbidity current ( <i>sensu</i> Lowe 1982).
	 High-density turbidite	 High-density turbidity current	Bed thickness 20-110 cm. Grain size: f-m, lesser coarse. Sedimentary structures: dominantly structureless (facies Sma).	Deposition from a high-density turbidity current ( <i>sensu</i> Lowe 1982).
	 Hybrid event bed (proximal)	 Hybrid flow (proximal)	Bed thickness: 40-200 cm, packages up to 18 m. Grain size: uvf-lm. Sedimentary structures: dominantly color banded (facies Sb), common dewatering structures, mud-clast-rich and mud-clast-poor examples. +/- argillaceous cap.	Deposition from flow which temporally fluctuated between relatively turbulent and cohesive states close to the bed (e.g., Baas et al. 2009).
	 Hybrid event bed (distal)	 Hybrid flow (distal)	Bed thickness: 25-200 cm. Grain size: uvf-lm. Sedimentary structures: wide range of facies - massive (Sma), laminated (Ss), color banded (Sb), and highly argillaceous unstratified sandstones (Smu). Mud-clast-rich and mud-clast-poor examples.	Deposition from flow in which the near-bed flow was relatively stable, but which varied longitudinally due to increasing down-dip concentration through deceleration and/or entrainment (e.g., Haughton et al. 2009; Baas et al. 2011).
	 Debrite	 Debris flow	Bed thickness: 20-65 cm. Grain size: f-m. Sedimentary structures: diamictic, plastic deformation – fold and shear structures.	Deposition from a debris flow (Lowe 1982).
Reworked deposits	 Bottom-current reworked sst	 Bottom current reworking	Bed thickness: 1-35 cm. Grain size: vf-f. Sedimentary structures: plane-parallel and ripple cross lamination (facies Ss), variable grading, internal erosion surfaces, sharp base and top.	Deep-water sediment-gravity-flow sands reworked by tractional currents attributed to bottom currents.
	 Tractional lag deposit	 Tractional lag	Bed thickness: 1 cm to packages of 2 m. Grain size: f-m. Sedimentary structures: weakly stratified (facies Sws), stratified (facies Ss), erosional remnants, lenticular, clean but with mud clasts, sharp base and top.	Winnowed tractional deposit formed at the base of a channel, scour, or bedform trough.

FIG. 2.—Bed-type classification with descriptions of typical characteristics and process-based interpretations. The principal bed types considered in this study are high-density turbidites (HDTs) and hybrid event beds (HEBs, proximal and distal types). Hybrid event beds are subdivided in this way due to their wide range of characteristics; it is noted that turbidity currents also undergo considerable longitudinal variability, i.e., proximal to distal trends, but in this case only high-density turbidity currents are considered important in a reservoir context. Figure partly modified from Haughton et al. 2009.

packages of tractional lag deposits which are suggestive of a relatively axial location. All proximal HEBs are characterized by dewatering structures, and in the Asterix sandstones such features are pervasive. Obelix is characterized by a predominance of proximal HEBs at its base, followed by a thick interval of proximal HEBs interbedded with HDTs, before returning to a thick interval of proximal HEBs towards the top. Farther down dip, the Gro wells are dominated by distinctly layered distal HEBs and lesser proximal HEBs and LDTs. The overall depositional environment, based on the bed-type distribution and overall downslope fining, is interpreted as a series of broadly progradational-to-retrograda-

tional and laterally stacked lobes characterized by HDTs in proximal areas and HEBs in distal and marginal areas (e.g., Hodgson et al. 2006; Hodgson et al. 2016; Haughton et al. 2009; Prélat et al. 2009).

**Petrographic Composition**

**Detrital Grains.**—The studied sandstones comprise quartz arenites and more rarely subarkoses composed of quartz, K-feldspar, plagioclase, mica, heavy minerals, and rock fragments (Fig. 6, Appendix). In Gjallar, Asterix, and Obelix the Springar Formation is very quartz-rich and contains 43–



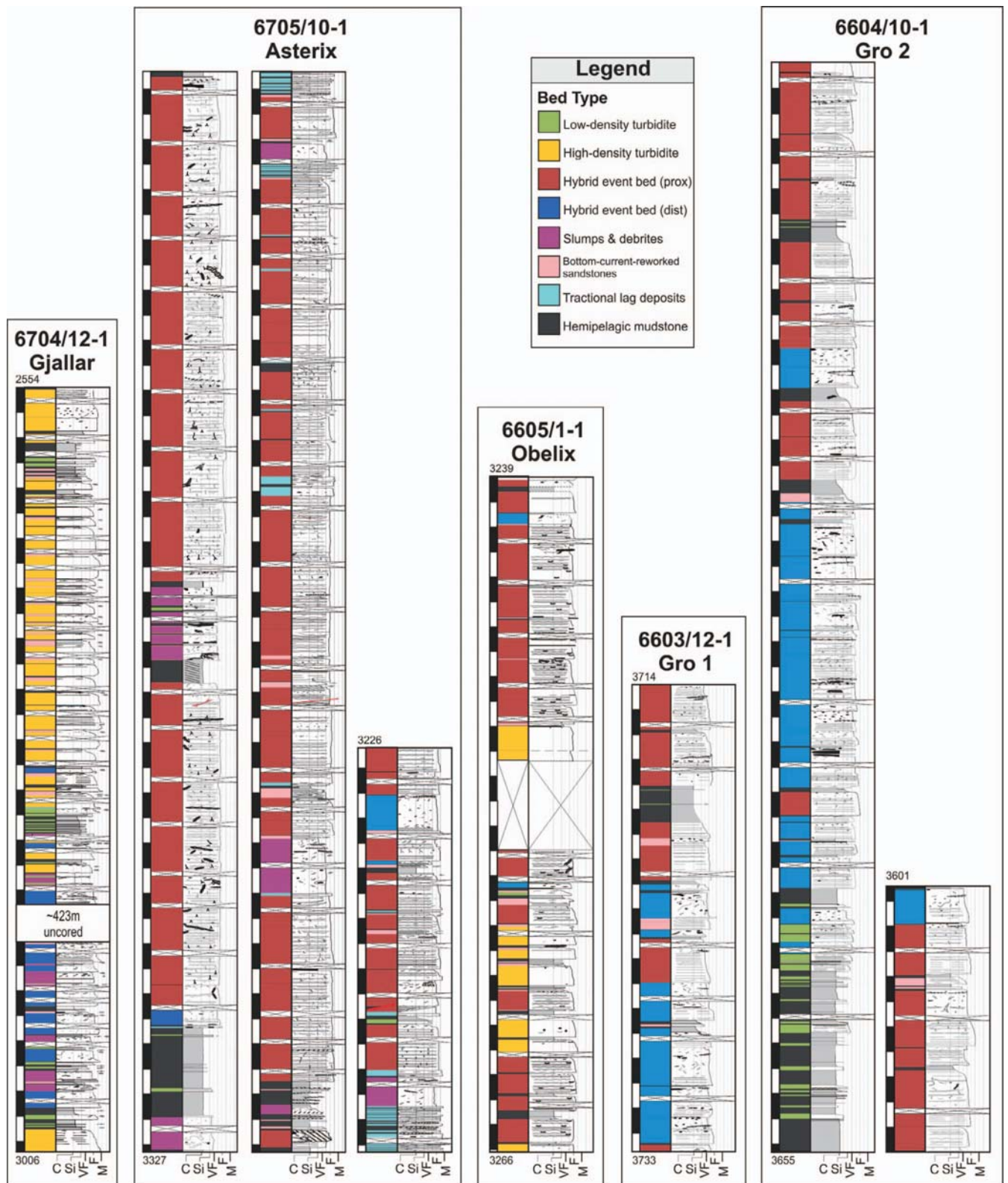


FIG. 3.—Sedimentary logs with bed-type distribution for the Springar interval in wells 6704/12-1 (Gjallar), 6705/10-1 (Asterix), 6605/1-1 (Obelix), 6603/12-1 (Gro 1), and 6604/10-1 (Gro 2). Scale in meters, top and bottom core depths in mRKB (meters below rotary table).

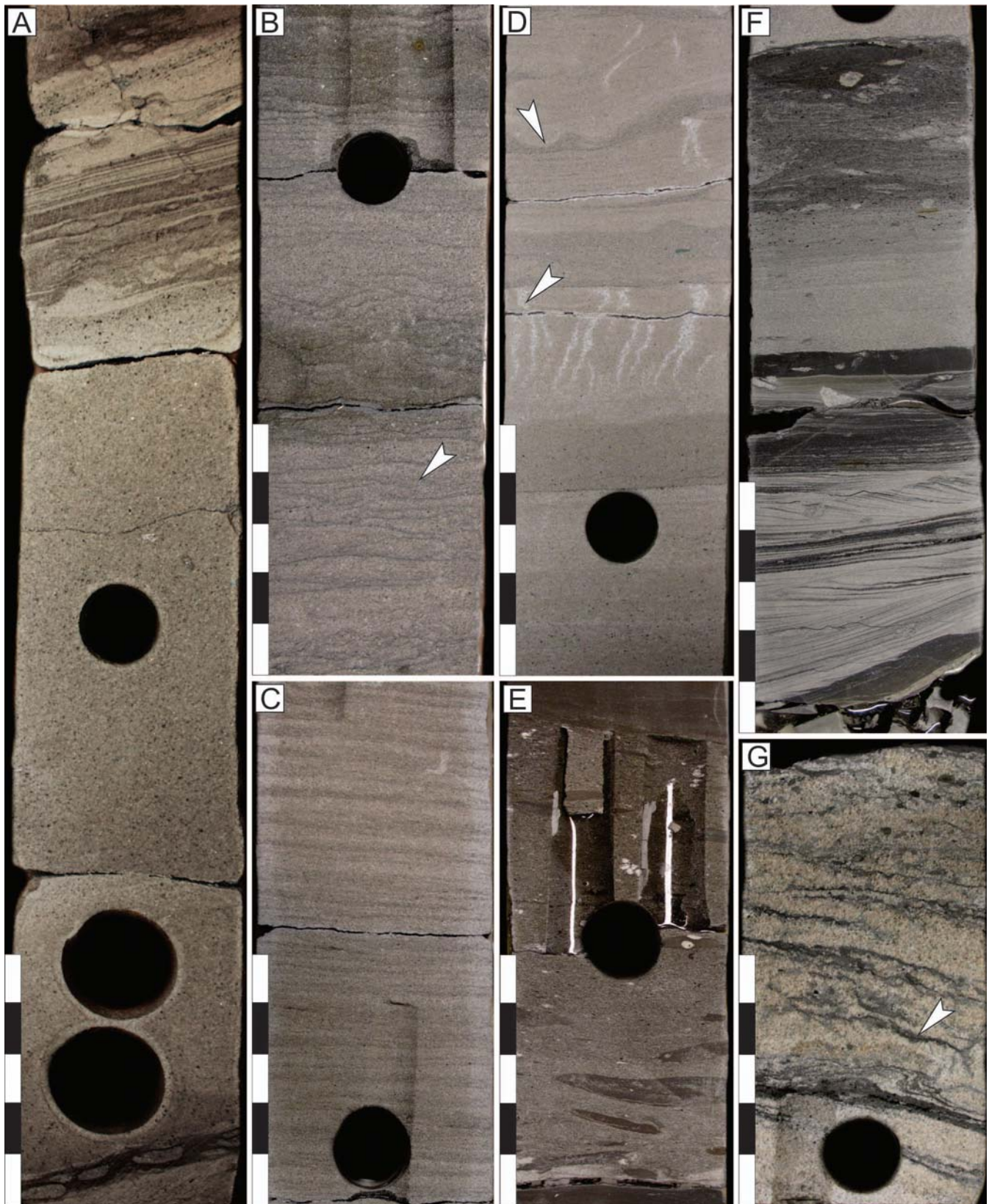


FIG. 4.—Photographs of principal bed types in the studied deep-marine fan system: **A**) high-density turbidite, **B**) proximal hybrid event bed with dish structures (arrow), **C**) proximal finely color-banded hybrid event bed, **D**) widely spaced color-banding in a hybrid event bed, with well-developed dewatering pipes (lower arrow) terminating at stylolitized boundary of dark band. Note the load structures marked by the upper arrow. **E**) Debrite with rounded clasts. **F**) Bottom-current-reworked sandstone in the lower half of the core, distal hybrid event bed in the upper part of the core. **G**) Tractional lag deposit with mud drapes (arrow). Scale bar is 10 cm.



67% detrital quartz corresponding to 75–97% of total detrital grains, whereas detrital quartz content in Gro 1 and Gro 2 samples is 38–69% or 65–92% of framework grains. K-feldspar and plagioclase contents of the Gjallar and Asterix wells are up to 2% and 1%, respectively. K-feldspar is not seen in samples from Obelix, and plagioclase (trace) is observed in one sample from this well. Only a few K-feldspar grains are observed in the Gro wells, whereas plagioclase content is relatively high with an average of 4% and a maximum of 8%. Muscovite, chert, heavy minerals, and glauconitic grains occur in trace amounts to a few percent each in all samples. Biotite (trace) is observed in a few samples from the Gjallar and Asterix wells, and in most of the Gro 1 and Gro 2 samples. Rock fragments (trace to 2%) and plant fragments (trace to 3%) occur in about sixty percent of the investigated samples. Clay clasts are present in trace volumes to 2% in the sandstones, but larger volumes occur, especially in samples from Gro 1 and Gro 2 (up to 17%). Detrital clay matrix consisting of interlocking particles without distinct crystal shapes, and with sizes mostly less than 10  $\mu\text{m}$ , is present in all samples from the Gjallar (5–10%), Asterix (1–10%), Obelix (6–9%), Gro 1 (7–10%), and Gro 2 (6–12%) wells. In the polarization microscope the clay matrix is characterized as a dark, pore-filling, and microporous mass (Fig. 6). SEM analysis of the detrital clay indicates that the matrix is probably a mixture of smectitic, illitic, and kaolinitic material (Fig. 7). Traces of chlorite may possibly be present.

**Diagenetic Minerals.**—Quartz cement is the most common diagenetic mineral in the Springar samples and accounts for up to 6% of sample volumes (Fig. 6, Appendix). These values include minor volumes of recycled quartz cement from older sandstones (trace to 2%). However, strongly quartz-cemented patches are observed where detrital clay does not cover quartz grains in the deepest Springar Formation samples in Gro 1 and Gro 2. Minor volumes of scattered siderite (trace to 3%), ankerite (trace to 5%), calcite (trace to 7%), and dolomite (trace) cement patches are also present. In a few of the samples poikilotopic calcite and microcrystalline siderite cements are present in volumes of 9–39%. These carbonate-rich samples have been excluded from the dataset where relationships between original sediment texture and reservoir properties are investigated. Pyrite framboids in detrital clay matrix (trace to 4%, Fig. 7A) and stacks of pseudohexagonal authigenic kaolin platelets (trace to 3%, Fig. 7C) occur in most samples, and traces of authigenic albite in dissolution pores are seen in about half of the samples.

**Texture.**—Overall, samples are grain-supported with some detrital clay matrix and preferred orientation of elongate grains, although dewatering has distorted the orientation of grains somewhat. Dominant grain size and detrital-clay volumes vary according to position along the depositional profile, and with respect to sandstone bed type (Fig. 6, Appendix). Samples from the Gjallar, Asterix, and Obelix wells are fine- to medium-grained sandstones (0.15–0.36 mm) and moderately to moderately well sorted. Gro 1 and Gro 2 samples are very fine- to upper fine-grained (0.06–0.23 mm, with the exception of one sample of 0.26 mm), and moderately to well sorted. Contents of detrital clay matrix, clay clasts, and glauconitic clasts increase from proximal to distal locations. These three components make up the class “total detrital clay” in Figure 6. Volumes of total detrital clay are not calculated for the strongly carbonate-cemented samples where detrital clay matrix was difficult to differentiate from cement. In Gjallar, Asterix, and Obelix total-detrital-clay content is within the range 5% to 16%, and twenty-five percent of the samples have volumes larger than

10%. In Gro 1 and Gro 2 total-detrital-clay content is higher, ranging from 8% to 26%, with about sixty percent of the samples having volumes larger than 10%.

Significant textural variations are also observed with respect to sandstone type (Fig. 6). HDTs have the coarsest grain size of the studied bed types, ranging from 0.18 mm to 0.36 mm (upper fine- to medium-grained). The proximal HEBs show a large span in grain sizes from 0.11 mm to 0.31 mm (upper very fine- to lower medium-grained). The distal HEBs generally have lower grain sizes than the HDTs and proximal HEBs, in the range of 0.12–0.21 mm (lower and upper fine-grained). Some larger and smaller grain sizes also occur for the distal HEBs (range 0.06 mm to 0.27 mm). Although variable between wells, total-detrital-clay content is higher in HEBs (5–26%) than in HDTs (6–10%, average 7%). Moreover, proximal HEBs have less total detrital clay (5–16%; almost eighty percent of the samples in the range 5–10%) than distal HEBs (8–26%; sixty percent of the samples have more than 10% total detrital clay). The sorting of samples from the various bed types is similar. HDTs and proximal HEBs are mainly moderately to moderately well sorted, while distal HEBs are mostly moderately well sorted.

### Porosity and Permeability

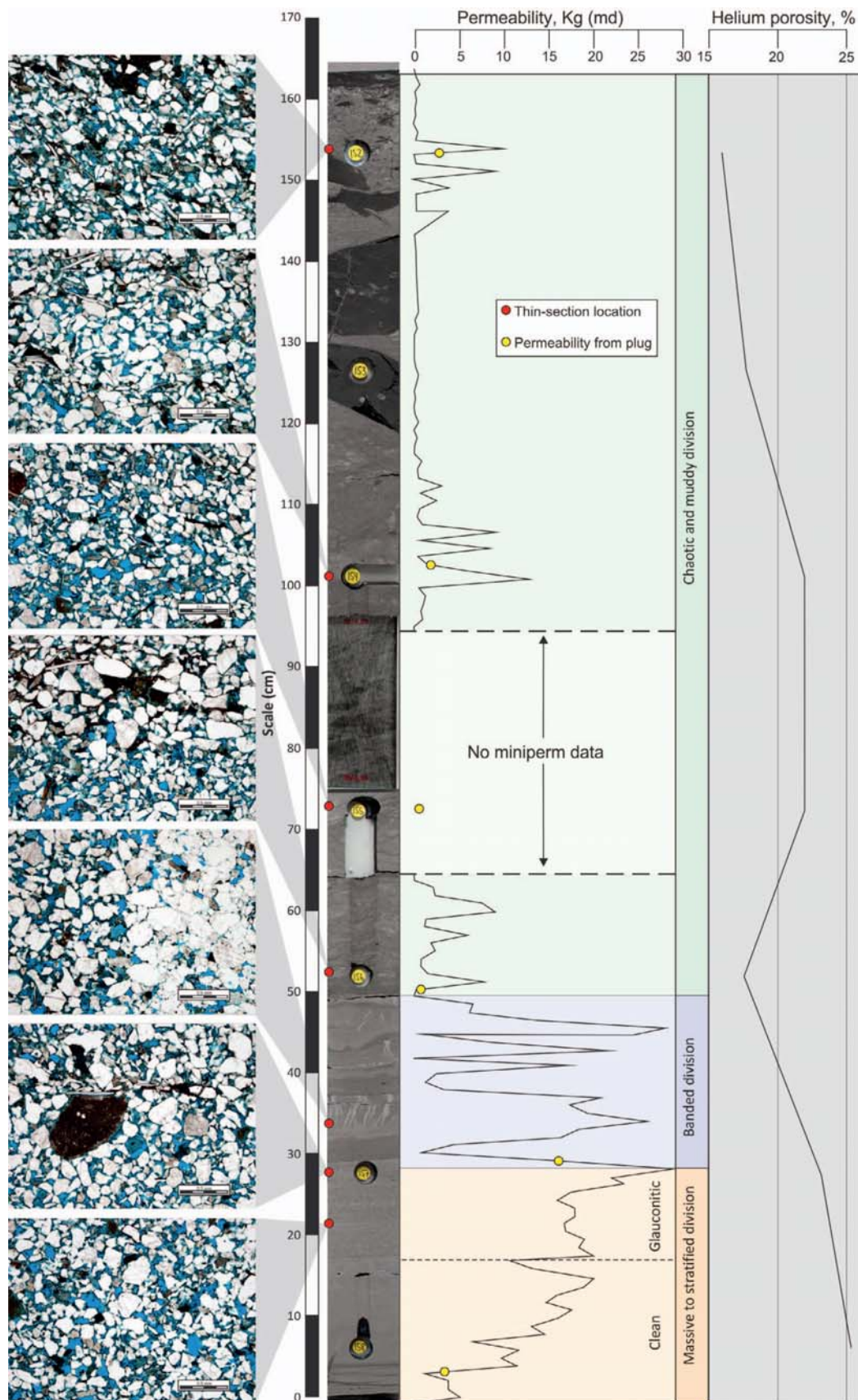
Figure 8 shows porosity and permeability versus depth below seafloor for the Springar Formation in the five investigated wells. There is a slight reduction in porosity of a few percent from the shallowest investigated interval in the Gjallar well, at ca. 1200 m, to the deepest interval in the Gro 1 well, at ca. 2300 m, and a clear reduction of permeability with burial depth from the Asterix interval (ca. 1900 m) to the Gro 1 sandstones.

Porosities and permeabilities of the Springar Formation are ca. 5% to 30% and from about 0.01 md to around 1500 md, respectively (Fig. 9A). The best reservoir properties are encountered in the Gjallar and Asterix wells, which have a significant fraction of samples with permeabilities two orders of magnitude higher than those of the same porosity values from the Obelix, Gro 1, and Gro 2 wells. However, both the Gjallar and Asterix wells also have groups of samples corresponding to the lower permeability–porosity trend of the three most distal wells in the Gjallar–Gro transect. Samples with porosities less than 10% and permeabilities less than 0.1 md are from strongly carbonate-cemented intervals.

Figure 9B shows horizontal gas permeability versus helium porosity for the plugs with corresponding thin sections investigated for the Gjallar, Asterix, Obelix, Gro 1, and Gro 2 wells. Porosities range from 13% to 30% and permeabilities from 0.1 md to 1300 md, and include the lower and upper parallel trends observed in Figure 9A. The lower trend has porosities of 13–29% and permeabilities of about 0.1–120 md, while the upper trend is dominated by the upper half of the spanned porosity interval (20–30%), with permeabilities of 40–1300 md; values which are approximately one to two orders of magnitude greater than those corresponding to identical porosity values of the lower permeability–porosity trend. The Gjallar samples dominantly show very good porosities and permeabilities of 27–30% and 410–1300 md, respectively, but there are also two samples with somewhat lower porosities (21% and 24%) and much lower permeabilities (1 md and less). Asterix is dominated by a linear trend of samples with porosities of 20–30% and corresponding permeabilities of about 40–500 md, but a few samples in this porosity interval have permeabilities less than 10 md and two samples with about 18% porosity have permeabilities of 752 md and 4 md. Porosity values in the Obelix well range from 19% to 29% and permeabilities are in the range of 4 md to 123 md, with one

Fig. 5.—Example of a thick hybrid event bed (distal type) with distinct internal divisions, from the Gro 2 core. The lowermost massive to stratified division shows a clear increasing-upwards permeability trend, with a negative kick at the lower boundary of a glauconitic section, then continued increase. The color-banded sandstone division has a saw-tooth profile in response to the clearly alternating clean (light) and clay-rich (dark) bands. The overlying chaotic and muddy division has generally low permeability with occasional spikes in response to cleaner sand patches. Log scale in centimeters, scale bar in micrographs is 0.5 mm.







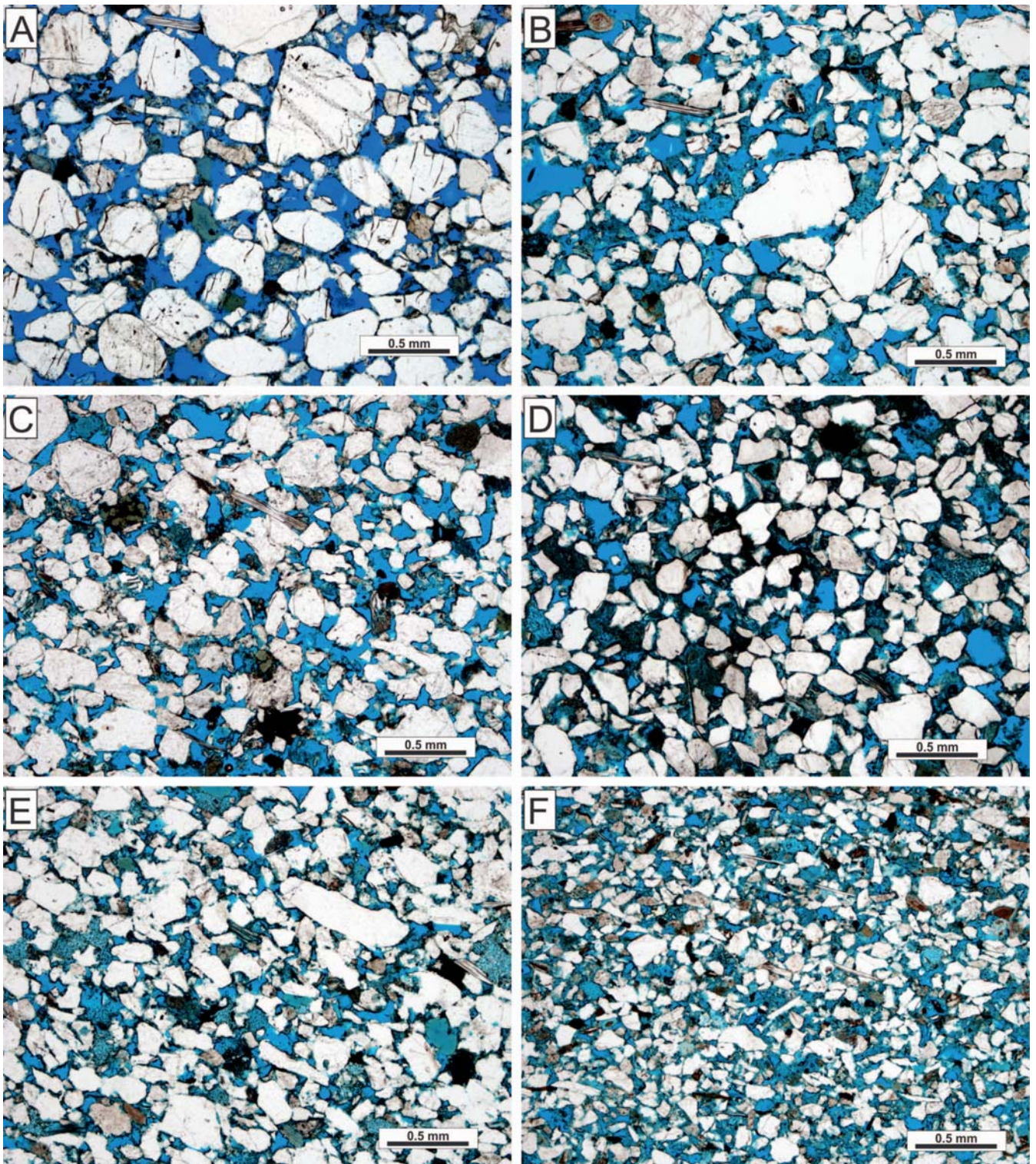


FIG. 6.—Examples of texture and composition of Springar Formation sandstones. Quartz and feldspars are white, detrital clay appears greenish, clay clasts are brown, and pores are blue: **A)** moderately sorted and medium-grained HDT with 6% total detrital clay concentrated in thin layers along grain surfaces, 28% porosity, and 700 md permeability (2560.85 mRKB, Gjallar well), **B)** moderately well sorted and upper fine-grained HDT with 8% total detrital clay dispersed in pores, 26% porosity, and 32 md permeability (3262.00 mRKB, Obelix well), **C)** moderately well sorted and upper fine-grained proximal HEB with 7% total detrital clay concentrated in thin layers along grain surfaces, 25% porosity, and 485 md permeability (3233.05 mRKB, Asterix well), **D)** well sorted and upper fine-grained proximal HEB with 11% total detrital clay dispersed in pores, 27% porosity, and 8 md permeability (3255.00 mRKB, Obelix well), **E)** moderately well sorted and upper fine-grained distal HEB with 10% total detrital clay dispersed in pores, 22% porosity, and 1 md permeability (3730.00 mRKB, Gro 1 well), and **F)** moderately well sorted and lower fine-grained distal HEB with 14% total detrital clay dispersed in pores, 17% porosity, and 0.1 md permeability (3624.00 mRKB, Gro 2 well).



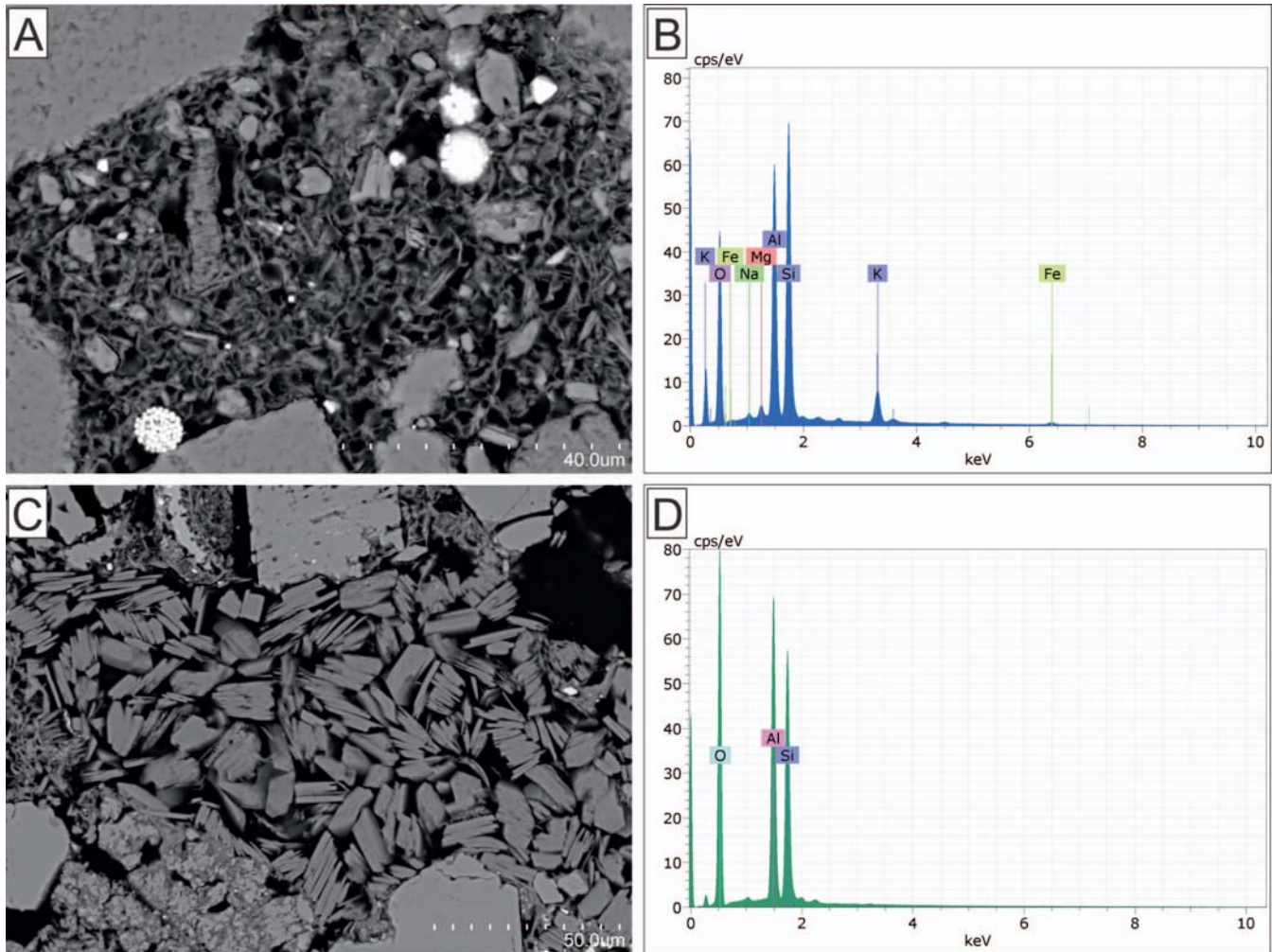


FIG. 7.—SEM micrographs and spectra for A, B) detrital clay matrix and C, D) authigenic kaolin. The detrital clay matrix is characterized by A) pore-filling or pore-lining small clay crystals (mostly less than 10  $\mu\text{m}$ ) without distinct shapes occurring in a mass together with silt grains and in places with framboidal pyrite, and by B) a multipeak elemental signal that most likely is a mixture of the signatures of smectite, illite, kaolin, and possibly traces of chlorite. The detrital clay matrix is in places contaminated by barite from drilling mud (sulfur peak at 2.3 keV), while the small chlorine peak at 2.6 keV is from the thin-section epoxy. The authigenic kaolin is easy to recognize from its C) rather large (5–20  $\mu\text{m}$ ) stacks of pseudo-hexagonal platelets restricted to single or a few adjoining pores, and D) its simple elemental signal.

sample outside this range at 13% porosity and 0.1 md permeability. Gro 1 has porosities of 17–24% and permeabilities of 0.2–10 md, whereas Gro 2 shows a slightly larger spread in reservoir properties with porosities of 16–28% and permeabilities of 0.1–15 md, with the exception of a strongly calcite-cemented sample (4% porosity and less than 0.01 md permeability).

To determine the effect of sediment-gravity-flow type on reservoir quality, the data on porosity and permeability shown in Figure 9A were compared to the inferred transport and depositional processes (defined in Fig. 2). Figure 9C clearly indicates that HDTs have the best reservoir properties in the studied Springar interval. Proximal HEBs have variable reservoir properties corresponding to the two main permeability–porosity trends of the dataset, while the distal HEBs, although variable, overall have lower porosity and permeability values than proximal HEBs. The low-density turbidites, reworked sandstones, and debrites have a range of reservoir properties corresponding to the lower permeability–porosity range of the distal HEBs. The tractional lag deposits fall on a linear permeability–porosity trend with permeabilities about one order of magnitude higher for a given porosity (350–13,000 md), than for the HDTs and the best proximal HEBs.

In Figure 9D permeability versus porosity with respect to bed type is shown for the plugs where thin sections are available. Strongly carbonate-cemented samples have here been excluded from the dataset to avoid the effect of early diagenesis on porosity and permeability. HDTs have very good porosities of 27–30% and permeabilities of 410–1300 md in Gjallar. One sample from a HDT in Obelix, falls outside this range with 26% porosity and 32 md permeability. The proximal HEBs have variable reservoir properties, with about half of the samples following the upper and the rest falling on the lower permeability–porosity trend. The upper trend of samples from proximal HEBs has very good porosities of 20–30% and permeabilities of ca. 40–500 md, whereas the samples in the lower proximal HEB trend are in the same porosity interval but have corresponding permeabilities about one order of magnitude less than the upper group of proximal HEB samples (ca. 3–100 md). The lower part of the proximal HEB trend (20–25% porosity, 5–10 md permeability) overlaps with the group of samples from distal HEBs that have the best reservoir properties. Porosities of distal HEBs span the range 13–28% and permeabilities are, with one exception (53 md), in the range 0.1 md to 15 md. One sample from a bottom-current-reworked sandstone and a

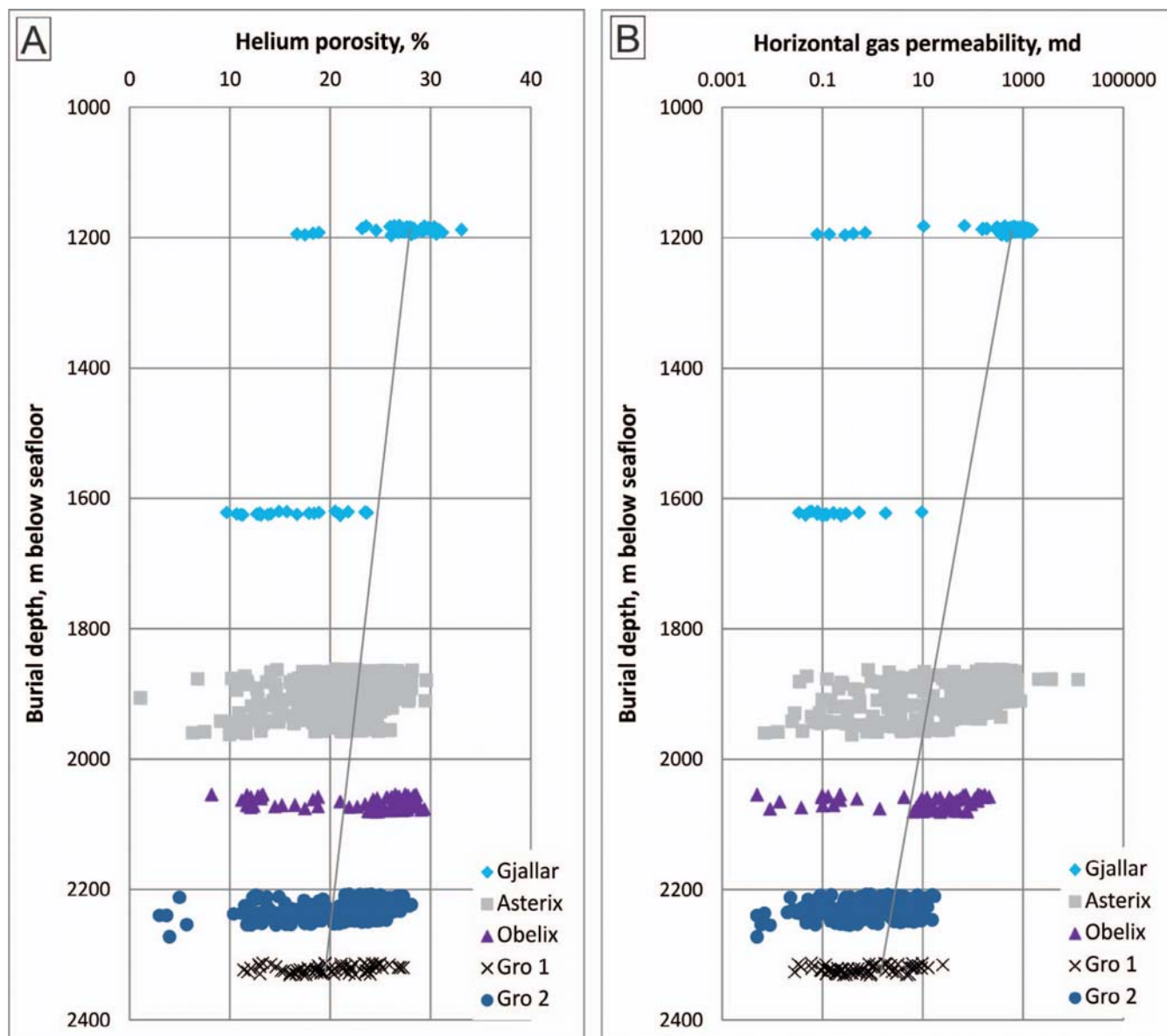


FIG. 8.—A) Porosity and B) permeability versus depth below seafloor for the Springar interval in wells 6704/12-1 (Gjallar), 6705/10-1 (Asterix), 6605/1-1 (Obelix), 6603/12-1 (Gro 1), and 6604/10-1 (Gro 2). Line connects the mean value for each well, excluding the lower interval of Gjallar.

tractional lag deposit has 21% porosity and 1 md permeability and 18% porosity and 752 md permeability, respectively.

The Springar Formation porosity and permeability data are illustrated with respect to their corresponding sedimentary facies (Fig. 9E, F). There is a large range in values for the various facies, but some general comments can be made. Unstratified sandstones mostly have good to very good porosity and permeability, 20–30% and 10–1500 md respectively. Weakly stratified sandstones mainly have good to very good porosity (20–27%) and moderate to very good permeability (2–600 md). Stratified and color-banded sandstones have very variable reservoir properties, with moderate to very good porosity (10–30%) and poor to very good permeability (0.03–13,000 md). Highly argillaceous unstratified sandstones mostly have moderate to good porosity (10–25%) and poor to moderate permeability (less than 10 md). Massive and laminated mudstones have moderate porosity (10–15%) and permeability less than 1 md.

DISCUSSION

*Controls on Reservoir Properties*

Quartz cementation is normally the most important diagenetic process and the main influence on reservoir quality in deeply buried quartz-rich sandstones (e.g., Blatt 1979; McBride 1989; Bjørlykke et al. 1989; Ehrenberg 1990; Walderhaug 1994a, 1994b; Walderhaug et al. 2000). The Springar Formation samples are from relatively shallow depths, 1.2–2.3 km below the seafloor, and they are presently at their maximum burial depth (Fig. 8). Volumes of quartz cement are less than 6% of sample volumes and therefore have not seriously reduced reservoir quality. However, strongly quartz-cemented patches are observed where clay matrix does not cover quartz-grain surfaces in the deepest Springar samples, suggesting that larger quartz-cement volumes and correspondingly lower porosities would have been present if quartz grains were not partially coated by detrital clay.



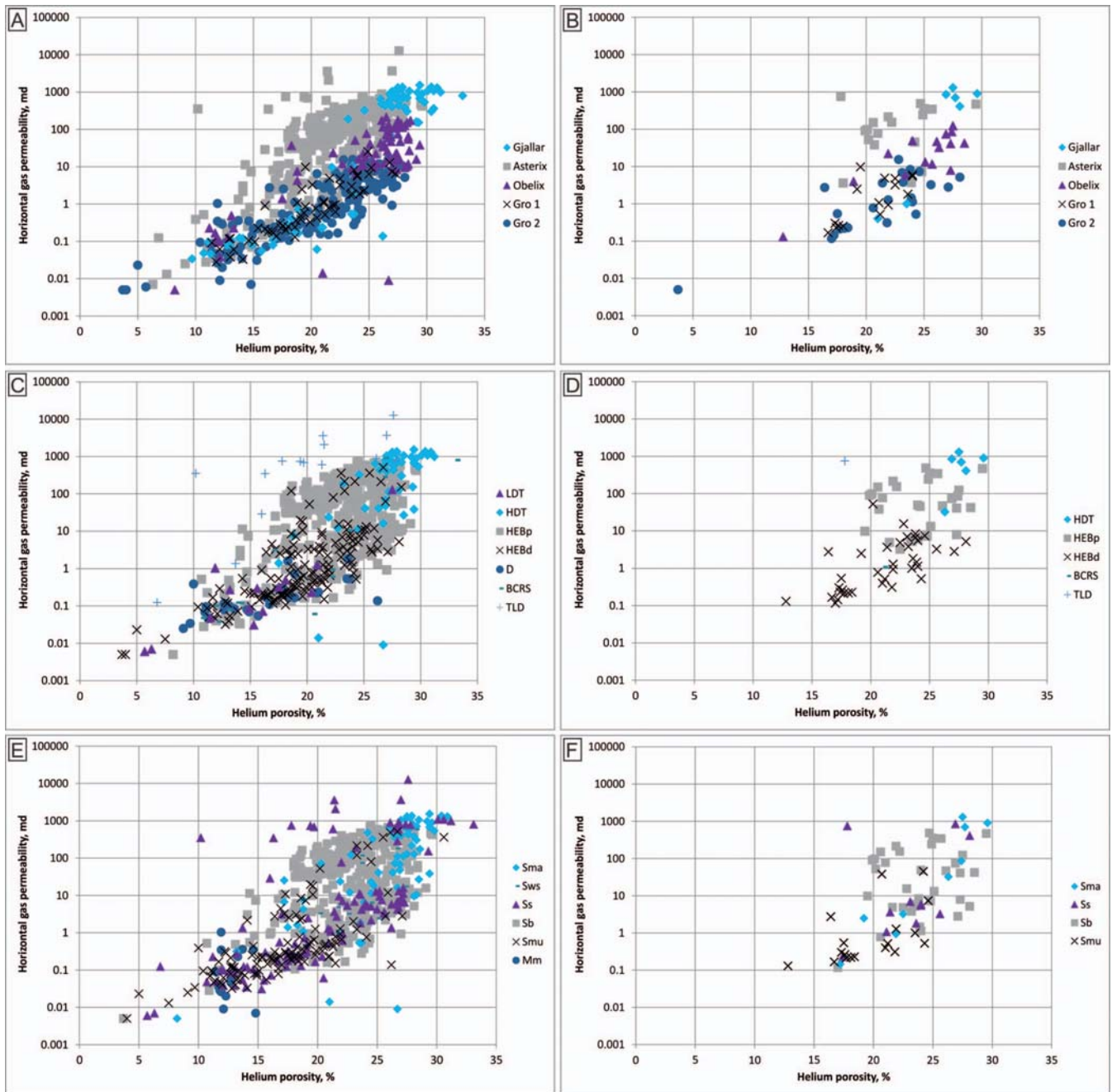


FIG. 9.—Horizontal gas permeability versus helium porosity for all 909 available plug measurements (left), and for the 82 plugs used for thin-section preparation (right) from the Springar interval, with respect to **A, B**) wells: 6704/12-1 (Gjallar), 6705/10-1 (Asterix), 6605/1-1 (Obelix), 6603/12-1 (Gro 1), and 6604/10-1 (Gro 2); **C, D**) bed types: LDT, low-density turbidite; HDT, high-density turbidite; HEBp, proximal hybrid event bed; HEBd, distal hybrid event bed; D, debris; BCRS, bottom-current-reworked sandstone; and TLD, tractional lag deposit; and **E, F**) sedimentary facies: Sma, massive sandstone; Sws, weakly stratified sandstone; Ss, stratified sandstone; Sb, color-banded sandstone; Smu, highly argillaceous unstratified sandstone; and Mm, massive and laminated mudstones. Samples with less than 10% porosity and 0.1 md permeability are from strongly calcite-cemented intervals and have together with other strongly carbonate-cemented samples been excluded from plots D and F which shows permeability versus porosity with respect to bed type and sedimentary facies, respectively, for the 74 plugs with thin sections showing minor to moderate diagenetic overprint.

Clay coats on quartz grains have, in numerous studies, been documented to inhibit quartz cementation (e.g., Heald and Larese 1974; Houseknecht and Ross 1992; Pittman et al. 1992; Ehrenberg 1993; Anjos et al. 2003).

Due to the moderate and similar diagenetic overprint of the sandstones (with the exception of the strongly carbonate-cemented samples), the observed differences in reservoir properties must be a result of primary

composition and texture (collectively termed the “depositional reservoir quality”) and possibly also variable mechanical compaction. Mechanical compaction occurs by grain rearrangement of mechanically stable grains and by plastic deformation of ductile grains (Houseknecht 1987; Wilson and Stanton 1994). Experimental studies demonstrate how porosity loss is accelerated in sands rich in clay matrix and clay clasts compared to matrix-

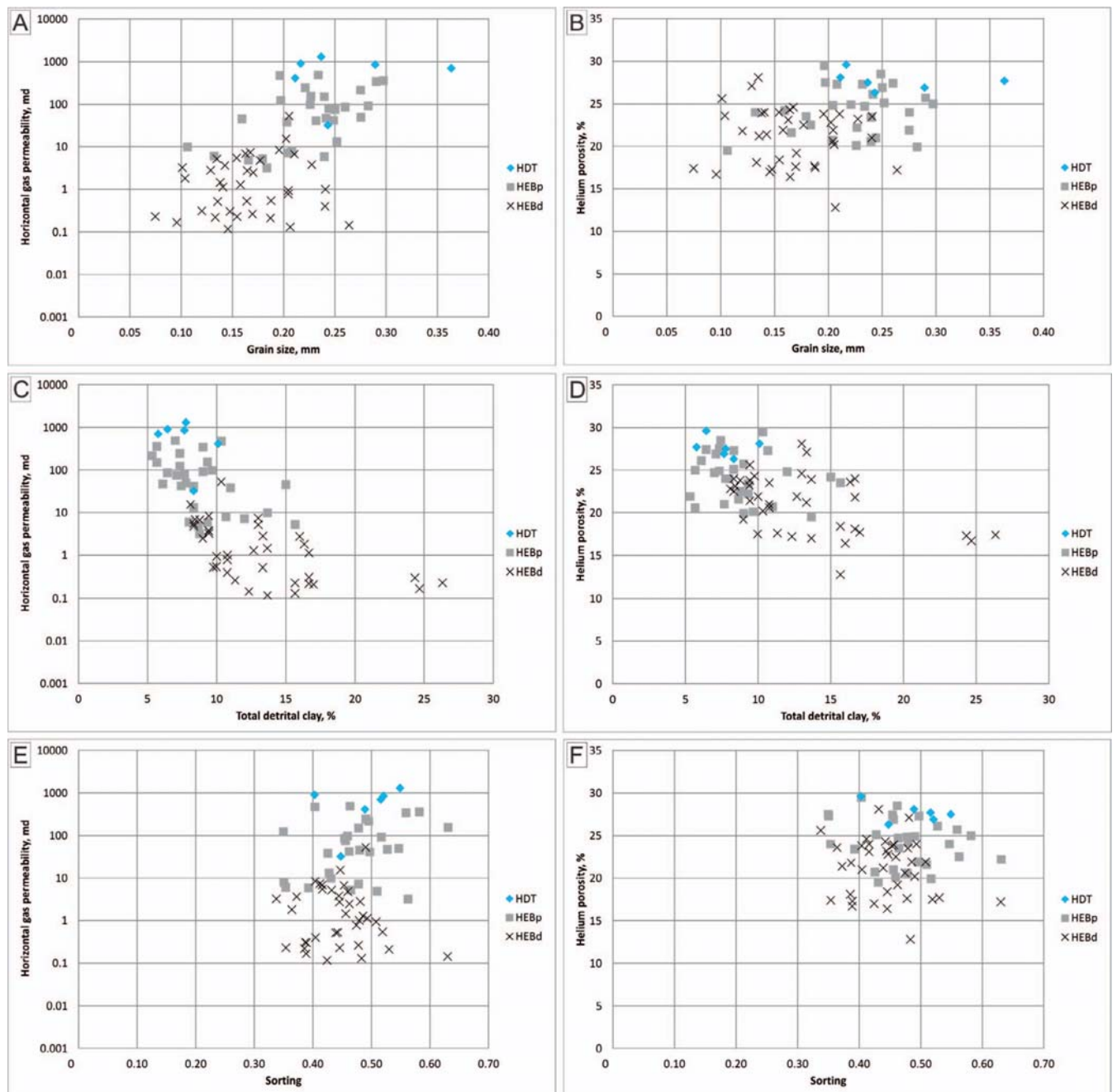


FIG. 10.—Permeability and porosity versus **A, B**) grain size, **C, D**) total detrital clay, and **E, F**) sorting, with respect to bed type (HDT, high-density turbidite; HEBp, proximal hybrid event bed; HEBd, distal hybrid event bed). Strongly siderite- and calcite-cemented samples and bed types with only one sample each are excluded (compare with Fig. 9D).

poor and quartz-rich sands (Pittman and Larese 1991). Porosity loss by mechanical compaction is therefore likely more pronounced for sands in distal hybrid event beds than in high-density turbidites and proximal hybrid event beds, as most of the proximal HEBs contain more than 10% ductile material (detrital clay, clay clasts, micas, and glauconitic grains).

In Figures 10 and 11 the effect of sediment texture parameters on porosity and permeability are shown with respect to sandstone bed type and facies, respectively. Porosity in the poorly cemented samples of the dataset increases with decreasing total-detrital-clay content, whereas

permeability increases with increasing grain size and decreasing total-detrital-clay volume. In addition, permeability is strongly dependent on porosity (Fig. 9). A similar relationship between permeability, porosity, composition, and textural parameters has recently been described and quantified for quartz-rich sandstones regardless of their depositional environment (Walderhaug et al. 2012). Lack of clay or other matrix material between the sand grains making up the rock framework results in better porosity than in a sandstone where the pores are partially filled by clay. As the content of microporous clay matrix increases, a larger



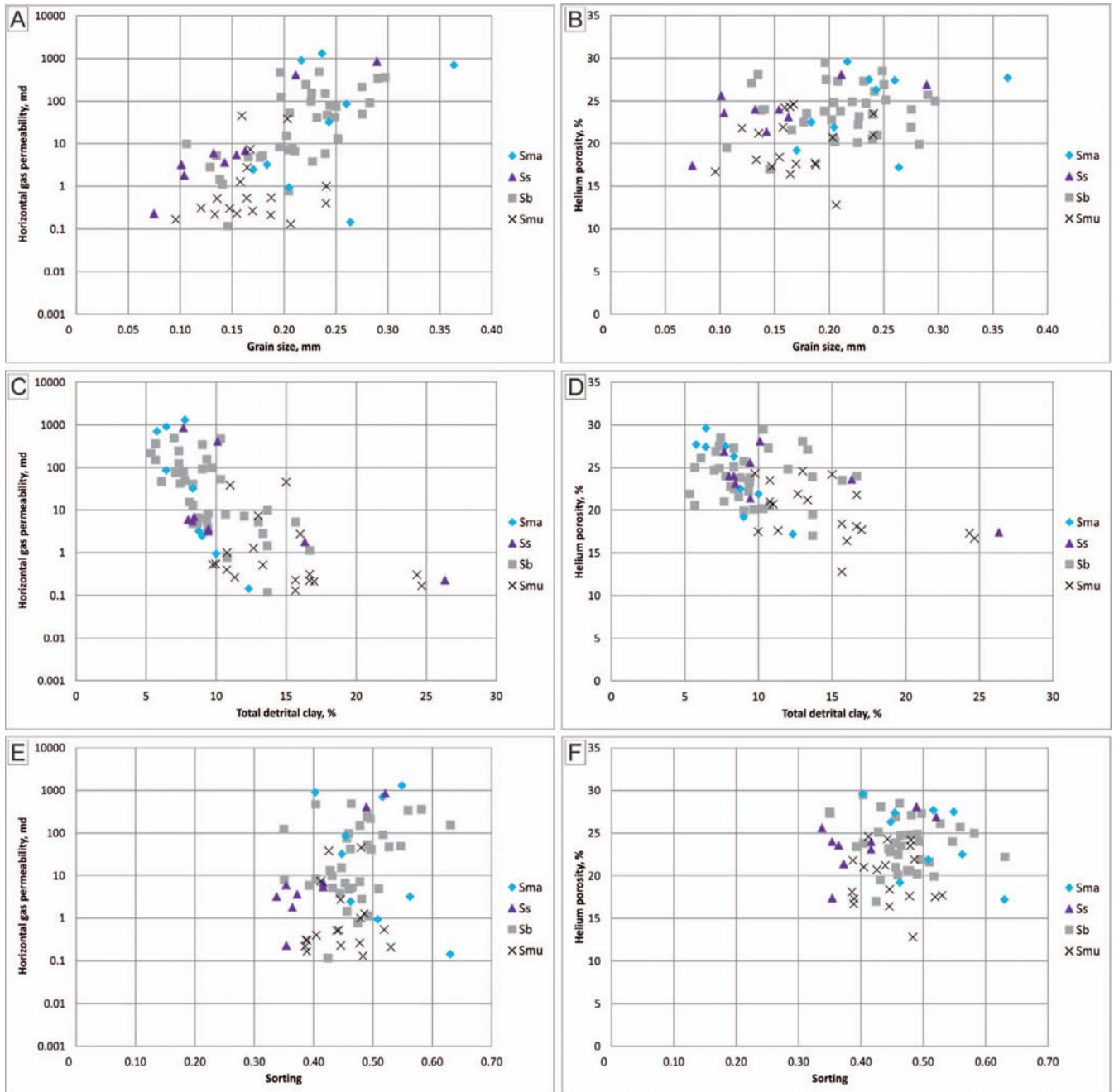


FIG. 11.—Permeability and porosity versus A, B) grain size, C, D) total detrital clay, and E, F) sorting, with respect to sedimentary facies (Sma, massive sandstone; Ss, stratified sandstone; Sb, color-banded sandstone; Smu, highly argillaceous unstratified sandstone). The data are the same as plotted in Figure 10.

proportion of the porosity becomes microporosity, and permeability drops significantly for a given porosity (e.g., Stalder 1973; Ehrenberg 1990; Ehrenberg and Boassen 1993; Midtbø et al. 2000; Walderhaug et al. 2012). Permeability increases with increasing grain size due to the presence of larger pore throats in coarser sands, whereas experimental work concludes that porosity is independent of grain size for sands of the same sorting (Beard and Weyl 1973). Similar to pore-filling clay, in poorly sorted sand small grains will fill spaces between larger grains and thus reduce porosity and permeability, compared to a situation where grains are of the same size (Beard and Weyl 1973). Clay-free, well sorted, and coarse-grained sands

consisting of mechanically strong grains consequently develop the most favorable reservoir properties. We were not able to distinguish any trends for porosity or permeability with sorting, which may be due to the more important effects of grain size and clay content on reservoir properties obscuring any influence of sorting.

Porosity and permeability vary significantly for the various bed types, due to variations in their detrital-clay content and dominant grain size (Figs. 9C, D, 10). The HDTs have the highest measured porosities and permeabilities, which is to be expected as these deposits are characterized by lower total-detrital-clay content and coarser grain sizes than the other

studied bed types. The somewhat more clay-prone and finer-grained proximal HEBs have intermediate to high porosities and a large span of permeabilities. HEBs from the Asterix well have permeabilities two orders of magnitude larger for a given porosity than equivalent samples from the Obelix well, while grain size and total-detrital-clay content ranges for the two wells are very similar. This permeability variation for a specific porosity is due to the different distribution of detrital clay in deposits from the two wells. In Obelix samples, microporous detrital clay is more dispersed throughout the pore system than in samples from the Asterix well, where detrital clay occurs mainly as relatively condensed and thin layers lining framework grains (Fig. 6C, D). Less dispersed clay in the Asterix sandstones is probably related to extensive sediment dewatering recorded in the core; syndepositional dewatering reorganized primary dispersed clay, leaving coatings on the surface of framework grains, as described for other dewatered deep-marine sandstones (Hurst and Buller 1984; Houseknecht and Ross 1992). Therefore, reservoir properties of the proximal HEBs sampled in the Obelix and Gro wells are probably more representative of this deposit type than the heavily dewatered sandstones encountered in the Asterix well. The exception is a few of the deeper proximal HEB samples from Asterix, which are among the most clay-rich and finest-grained from the three most proximal wells of the Gjallar–Gro transect. These samples are from an interval with less macroscopic evidence of dewatering in core and have relatively homogeneously dispersed detrital clay in thin section. The porosities and permeabilities of distal HEBs fall within the lower to intermediate range of the dataset, which correspond to these deposits being the most clay-rich and finest-grained of the studied bed types. The one distal type HEB sample which falls on the upper permeability–porosity trend (Fig. 9C, D) is from the Asterix well and has a large proportion of its clay matrix as thin grain coatings, as do the proximal HEB samples from this well.

Low-density turbidites are volumetrically minor in the Springar Formation and were not described petrographically, but from our experience with other deep-water sandstone datasets and published work (Lien et al. 2006; Njoku and Pirmez 2011; Kilhams et al. 2012), LDTs are normally finer-grained and contain similar amounts or more total detrital clay than HDTs. The LDTs of the studied system are silty to very fine-grained sandstones, with plane-parallel and ripple cross lamination throughout (Fig. 2); suggesting that fine grain size and high detrital clay content are responsible for placing these deposits in the lower end of the permeability–porosity range of the dataset (Fig. 9C). The bottom-current-reworked sandstones have character and reservoir properties similar to LDTs. Debrites are coarser grained (fine to medium) but contain more detrital clay than LDTs, and resulting ranges in porosity and permeability are similar. The tractional lag deposits are mostly free of pore-filling matrix, providing them with excellent permeability, although some contain millimeters-thick mud clasts and compacted mud drapes which reduce porosity (e.g., sample 3242.00 mRKB Asterix well; see the Appendix and Figs. 4G, 9D).

Porosity and permeability are variable for the various sedimentary facies, inasmuch as the facies can have a range of grain sizes and total-detrital-clay volumes (Figs. 9E, F, 11). Overall, however, massive sandstones are typically coarser grained and contain less total detrital clay than stratified and highly argillaceous unstratified sandstones, and color-banded sandstones have a large range in grain sizes but mainly contain less total detrital clay than highly argillaceous unstratified sandstones. Comparing Figures 10 and 11 shows that variation in sediment facies, grain size, and total detrital clay is partly due to their occurrence in different deposit types, e.g., massive sandstones are coarser grained and contain less total detrital clay in high-density turbidites than in distal hybrid event beds. In addition, longitudinal fractionation of the constituent sediment in a gravity current can result in significant variability of grain size, shape, and clay content in a proximal-to-distal transect in individual beds.

### *Depositional Reservoir Quality of Deep-Marine Sandstones*

Depositional reservoir quality decreases significantly proximally to distally, and from axis to margin, across deep-marine lobes. Distal HEBs are likely to have permeabilities up to two orders of magnitude lower than equivalent-porosity HDTs, due to the less common occurrence of detrital clay matrix and clay clasts in the latter. Porosity ranges of the various studied bed types are similar, but HDTs overall have higher porosities than HEBs, as: 1) some porosity is filled by detrital clay in HEBs, and 2) higher volumes of ductile detrital clay matrix and clay clasts in HEBs have increased the degree of mechanical compaction compared to in HDTs. Also, distal HEBs typically have lower porosities and permeabilities than proximal HEBs, due to their higher total-detrital-clay content (matrix and clasts), and finer grain size, than the latter. Similar relationships between sediment texture of deep-marine sandstones and reservoir properties have previously been described by others (Marzano 1988; Lien et al. 2006; Ehrenberg et al. 2008; Njoku and Pirmez 2011; Kilhams et al. 2012; Marchand et al. 2015).

Figure 12 shows an idealized diagram of permeability–porosity trends for various deep-marine deposits, based on depositional process and sediment texture. The figure emphasizes: 1) how increasing volumes of ductile detrital-clay matrix and clay clasts result in decreasing porosities, 2) how increasing volumes of microporous detrital clay and decreasing grain size give lower permeabilities, and 3) how permeability–porosity trends of HEBs are shifted to permeability values orders of magnitude lower than for idealized turbidites (HDTs and LDTs). Notice that this schematic figure applies when evaluating reservoir properties for deposits with a common source area and minor diagenetic overprint, i.e., for a specific depositional system, formation, or area with a similar burial history.

The effect of increasing burial will shift the various sandstones towards lower porosities and permeabilities as a function of quartz cementation in the case of quartzose sandstones. The onset of quartz cementation on the Norwegian continental shelf has been shown to occur at temperatures of about 70–80°C (Bjørlykke et al. 1989; Ehrenberg 1990; Walderhaug 1994a; Walderhaug et al. 2000), and precipitation rate increases exponentially with temperature and linearly with quartz-grain surface area available for precipitation of quartz overgrowths (Walderhaug 1994b; 1996; 2000; Bjørkum et al. 1998; Walderhaug et al. 2000). Therefore, quartz cementation is more pronounced with: 1) increasing proportion of quartz grains in a sediment, 2) decreasing quartz grain size, and 3) decreasing degree of quartz grain coating by clays, soft grains, or calcite cements. Consequently, predictions of how various deep-marine sandstones lose porosity by quartz cementation with burial to increasing temperatures can be outlined (Fig. 13).

Porosity and permeability are high at the time of deposition, due to loose grain packing. Depositional porosities of sands from various depositional settings are in the range 40–55%, and are assumed to be reduced to 20–35% during mechanical compaction (review in Wilson and Stanton 1994). In highly quartzose and feldspathic sandstones, mechanical compaction occurs by rearrangement of grains by rotation and slippage into more stable packing positions, but if the contents of ductile grains significantly exceed 10%, plastic deformation by bending or squashing of grains becomes important or even dominant during mechanical compaction (Wilson and Stanton 1994). During mechanical compaction, porosity and permeability will thus decrease more rapidly for HEBs rich in soft detrital clay matrix and clay clasts than for turbidites (HDTs and LDTs) with minor soft clay matrix and clay clasts. After the onset of quartz cementation, clay-free and fine-grained sandstones will be most rapidly cemented, whereas coarse-grained sands and sands with significant amounts of pore-filling clay will contain smaller volumes of quartz cement at a given depth and time. Eventually, most porosity in clay-free sandstones will be filled by quartz cement, while clay-filled pores (i.e., microporosity) will remain uncemented.



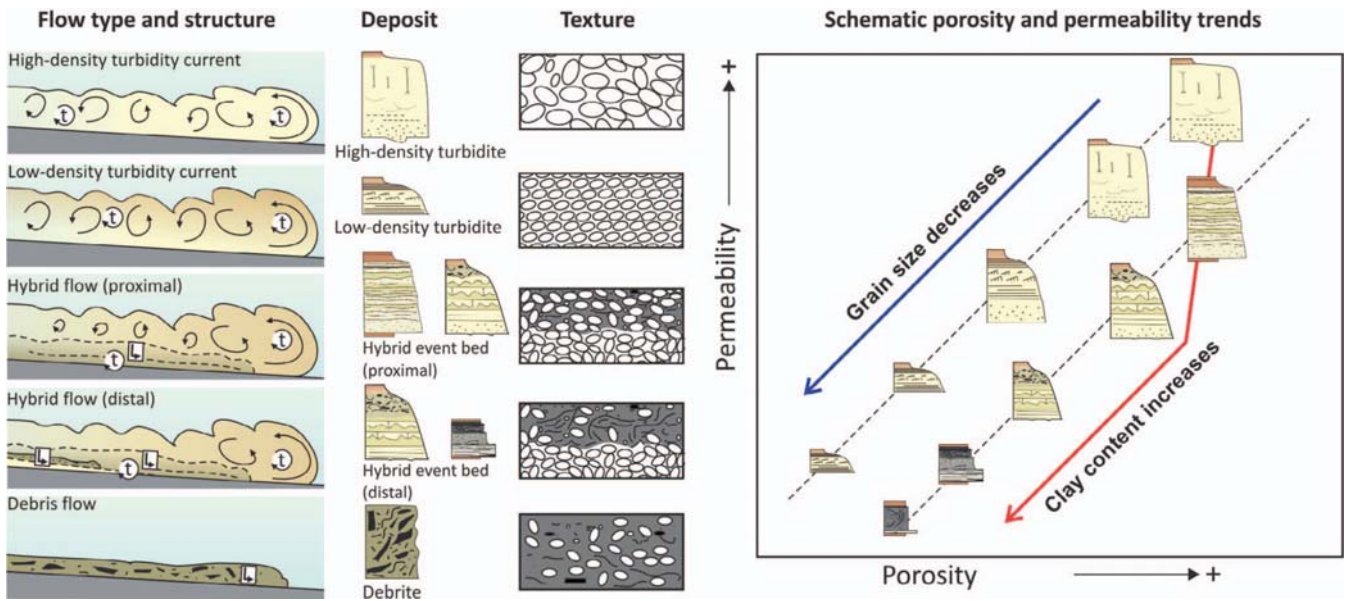


FIG. 12.—Schematic diagram illustrating the relationship between deep-marine flow mechanism, deposit, texture, and resultant reservoir properties in the Springar Formation. Hybrid event beds typically have permeability values two orders of magnitude lower than high- and low-density turbidites. The typical proximal to distal evolution of classical turbidites and hybrid event beds is illustrated on a permeability versus porosity plot. Debrites can have a wide range of grain sizes and textural properties, but they are usually matrix-rich with a significant detrital clay and clay-clast content.

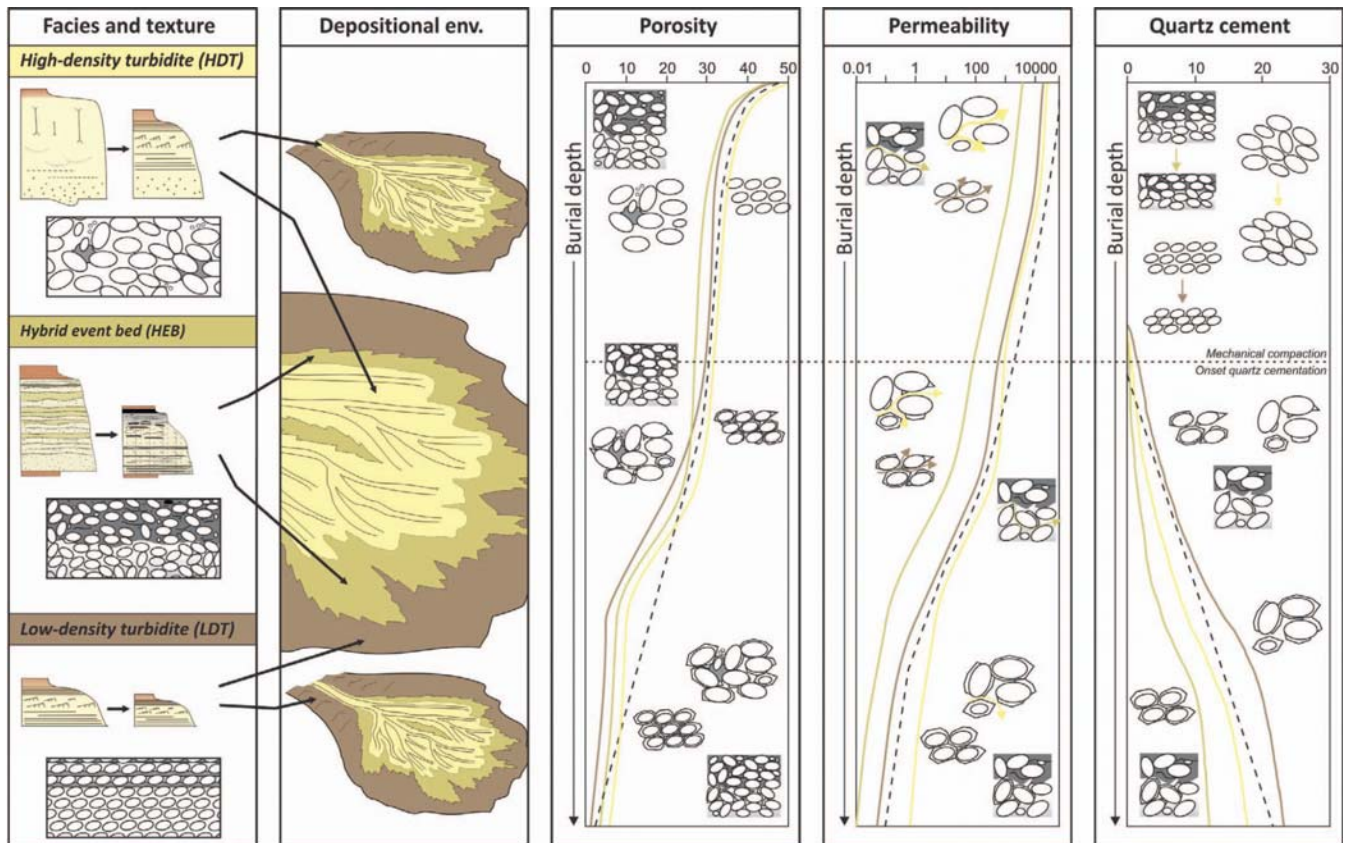


FIG. 13.—Conceptual model illustrating porosity, permeability, and quartz-cement development with burial for HDTs (yellow), HEBs (green), and LDTs (brown). The dashed line represents typical previously published depth trends for reservoir sandstones on the Norwegian continental shelf (e.g., Bjørlykke et al. 1989; Ehrenberg 1990; Ramm 2000). Variability in evolution of reservoir properties with burial is controlled by original sediment composition (especially grain size, sorting, detrital-clay content, and proportion of ductile grains) and quartz cementation (function of temperature history, quartz grain volume, grain size, and degree of quartz grain coating by clays etc.).

Thus, after severe quartz cementation, porosity in clay-rich HEBs might be higher than in turbidite deposits (HDTs and LDTs) at a given burial depth, but microporosity in matrix-filled uncemented pores typically contributes very little to permeability.

### CONCLUSIONS

Reservoir properties of weakly to moderately cemented Springar Formation deep-marine sandstones of the northwestern Vøring Basin are strongly influenced by original sediment composition, transport, and depositional histories. Porosity increases with decreasing total-detrital-clay content, and permeability increases with increasing grain size, decreasing total-detrital-clay volume, and increasing porosity. Clay-free, well sorted, and medium-grained high-density turbidites (HDTs) develop the most favorable reservoir rocks, and depositional reservoir quality decreases as detrital-clay content increases and/or grain size decreases for proximal and distal hybrid event beds (HEBs). Porosities of the various bed types span the same interval, but overall the HDTs and proximal HEBs have a larger proportion of samples with porosities higher than 20%, compared to the distal HEBs. Permeabilities, in contrast, are significantly different, with the HDTs having permeabilities approximately two orders of magnitude higher than clay-rich HEBs. Distinctive trends of porosity and permeability for the designated bed types support our interpretation that these are individual bed types formed by specific processes, and that there is a continuum of evolving processes from proximal to distal areas. Interpretation of the transport and depositional processes responsible for producing different bed types with characteristic composition and texture is an essential step in reservoir evaluation—necessary for predicting most likely evolution of porosity and permeability with sediment burial and for understanding distribution of reservoir quality in potential reservoir targets.

### SUPPLEMENTAL MATERIAL

An Appendix is available from JSR's Data Archive: <http://sepm.org/pages.aspx?pageid=229>.

### ACKNOWLEDGMENTS

This paper is based on projects performed for Statoil ASA, and Statoil's permission to publish is gratefully acknowledged. A/S Norske Shell and Rodmar Ravnås are thanked for providing permission and access to sample the Gro cores. The original manuscript was improved by the helpful comments of Olav Walderhaug and Simon Barker. We also thank referees Ann Marchand and William Morris, and Associate Editor David Hodgson, for their constructive reviews and comments.

### REFERENCES

- ANJOS, S.M.C., DE ROS, L.F., and SILVA, C.M.A., 2003, Chlorite authigenesis and porosity preservation in the Upper Cretaceous marine sandstones of the Santos Basin, offshore eastern Brazil, in Worden, R.H., and Morad, S., eds., *Clay Mineral Cements in Sandstones*: International Association of Sedimentologists, Special Publication 34, p. 291–316.
- BAAS, J.H., BEST, J.L., PEAKALL, J., and WANG, M., 2009, A phase diagram for turbulent, transitional and laminar clay suspension flows: *Journal of Sedimentary Research*, v. 79, p. 162–183.
- BAAS, J.H., BEST, J.L., and PEAKALL, J., 2011, Depositional processes, bedform development and hybrid bed formation in rapidly decelerated cohesive (mud–sand) sediment flows: *Sedimentology*, v. 58, p. 1953–1987.
- BARKER, S.P., HAUGHTON, P.D.W., McCAFFREY, W.D., ARCHER, S.G., and HAKES, B., 2008, Development of rheological heterogeneity in clay-rich high-density turbidity currents: Aptian Britannia Sandstone Member, U.K. continental shelf: *Journal of Sedimentary Research*, v. 78, p. 45–68.
- BEARD, D.C., and WEYL, P.K., 1973, Influence of texture on porosity and permeability of unconsolidated sand: *American Association of Petroleum Geologists, Bulletin*, v. 57, p. 349–369.
- BJØRKUM, P.A., OELKERS, E.H., NADEAU, P.H., WALDERHAUG, O., and MURPHY, W.M., 1998, Porosity prediction in quartzose sandstones as a function of time, temperature, depth, stylolites frequency, and hydrocarbon saturation: *American Association of Petroleum Geologists, Bulletin*, v. 82, p. 637–648.
- BJØRLYKKE, K., 2014, Relationships between depositional environments, burial history and rock properties. Some principal aspects of diagenetic process in sedimentary basins: *Sedimentary Geology*, v. 301, p. 1–14.
- BJØRLYKKE, K., RAMM, M., and SAIGAL, G.C., 1989, Sandstone diagenesis and porosity modification during basin evolution: *Geologische Rundschau*, v. 78, p. 243–268.
- BLATT, H., 1979, Diagenetic processes in sandstones, in Scholle, P.A., and Schluger, P.R., eds., *Aspects of Diagenesis*: SEPM, Special Publication 26, p. 141–157.
- BLOCH, S., 1994, Effect of detrital mineral composition on reservoir quality, in Wilson, M.D., ed., *Reservoir Quality Assessment and Prediction in Clastic Rocks*: SEPM, Short Course 30, p. 161–182.
- BLOCH, S., and MCGOWEN, J.H., 1994, Influence of depositional environment on reservoir quality prediction, in Wilson, M.D., ed., *Reservoir Quality Assessment and Prediction in Clastic Rocks*: SEPM, Short Course 30, p. 41–57.
- BREKKE, H., DAHLGREN, S., NYLAND, B., and MAGNUS, C., 1999, The prospectivity of the Vøring and More basins on the Norwegian Sea continental margin, in Fleet, A.J., and Boldy, S.A.R., eds., *Petroleum Geology of Northwest Europe*, Proceedings of the 5th Conference: Geological Society of London, p. 261–274.
- DAVIES, C., HAUGHTON, P., McCAFFREY, W., SCOTT, E., HOGG, N., and KITCHING, D., 2009, Character and distribution of hybrid sediment gravity flow deposits from the outer Forties Fan, Palaeocene Central North Sea, UKCS: *Marine and Petroleum Geology*, v. 26, p. 1919–1939.
- EHRENBERG, S.N., 1990, Relationship between diagenesis and reservoir quality in sandstones of the Garm Formation, Haltenbanken, mid-Norwegian continental shelf: *American Association of Petroleum Geologists, Bulletin*, v. 74, p. 1538–1558.
- EHRENBERG, S.N., 1993, Preservation of anomalously high porosity in deeply buried sandstones by grain-coating chlorite: examples from the Norwegian Continental Shelf: *American Association of Petroleum Geologists, Bulletin*, v. 77, p. 1260–1286.
- EHRENBERG, S.N., 1997, Influence of depositional sand quality and diagenesis on porosity and permeability: examples from Brent Group reservoirs, northern North Sea: *Journal of Sedimentary Research*, v. 67, p. 197–211.
- EHRENBERG, S.N., and BOASSEN, T., 1993, Factors controlling permeability variation in sandstones of the Garm Formation in Trestad field, Norwegian continental shelf: *Journal of Sedimentary Petrology*, v. 63, p. 929–944.
- EHRENBERG, S.N., NADEAU, P.H., and STEEN, Ø., 2008, A megascale view of reservoir quality in producing sandstones from the offshore Gulf of Mexico: *American Association of Petroleum Geologists, Bulletin*, v. 92, p. 145–164.
- FIJELLANGER, E., SURLYK, F., WAMSTEEKER, L.C., and MIDTUN, T., 2005, Upper Cretaceous basin-floor fans in the Vøring Basin, Mid Norway shelf, in Wandås, B.T.G., Nystuen, J.P., Eide, E.A., and Gradstein, F.M., eds., *Onshore–Offshore Relationships on the North Atlantic Margin*: Norwegian Petroleum Society, Special Publication 12, p. 135–164.
- FONNELAND, H.C., LIEN, T., MARTINSEN, O.J., PEDERSEN, R.B., and KOSLER, J., 2004, Detrital zircon ages: a key to understanding deposition of deep marine sandstones in the Norwegian Sea: *Sedimentary Geology*, v. 164, p. 147–159.
- FERSETH, R., and LIEN, T., 2002, Cretaceous evolution in the Norwegian Sea: a period characterized by tectonic quiescence: *Marine and Petroleum Geology*, v. 19, p. 1005–1027.
- FRASER, H.J., 1935, Experimental study of the porosity and permeability of clastic sediments: *Journal of Geology*, v. 43, p. 910–1010.
- HAUGHTON, P.D.W., BARKER, S.P., and McCAFFREY, W.D., 2003, “Linked” debrites in sand-rich turbidite systems: origin and significance: *Sedimentology*, v. 50, p. 459–482.
- HAUGHTON, P., DAVIS, C., McCAFFREY, W., and BARKER, S., 2009, Hybrid sediment gravity flow deposits: classification, origin and significance: *Marine and Petroleum Geology*, v. 26, p. 1900–1918.
- HEALD, M.T., and LARESE, R.E., 1974, Influence of coatings on quartz cementation: *Journal of Sedimentary Petrology*, v. 44, p. 1269–1274.
- HODGSON, D., 2009, Distribution and origin of hybrid beds in sand-rich submarine fans of the Tanqua depocentre, Karoo Basin, South Africa: *Marine and Petroleum Geology*, v. 26, p. 1940–1956.
- HODGSON, D.M., FLINT, S.S., HODGETTS, D., DRINKWATER, N.J., JOHANNESSEN, E.P., and LUTHI, S.M., 2006, Stratigraphic evolution of fine-grained submarine fan systems, Tanqua Depocenter, Karoo Basin, South Africa: *Journal of Sedimentary Research*, v. 76, p. 20–40.
- HODGSON, D., KANE, I., FLINT, S., BRUNT, R., and ORTIZ-KARPE, A., 2016, Time transgressive confinement on the slope and the progradation of basin-floor fans: implications for the sequence stratigraphy of deep-water deposits: *Journal of Sedimentary Research*, v. 86, p. 73–86.
- HOUSEKNECHT, D.W., 1987, Assessing the relative importance of compaction processes and cementation to reduction of porosity in sandstones: *American Association of Petroleum Geologists, Bulletin*, v. 71, p. 633–642.
- HOUSEKNECHT, D.W., and ROSS, L.M., JR., 1992, Clay minerals in Atokan deep-water sandstone facies, Arkoma Basin: origins and influence on diagenesis and reservoir quality, in Houseknecht, D.W., and Pittman, E.D., eds., *Origin, Diagenesis, and Petrophysics of Clay Minerals in Sandstones*: SEPM, Special Publication 47, p. 227–240.



- HURST, A., AND BULLER, A.T., 1984, Dish structures in some Paleocene deep-sea sandstones (Norwegian sector, North Sea): origin of the dish-forming clays and their effect on reservoir quality: *Journal of Sedimentary Petrology*, v. 54, p. 1206–1211.
- KANE, I.A., AND PONTÉN, A.S.M., 2012, Submarine transitional flow deposits in the Paleogene Gulf of Mexico: *Geology*, v. 40, p. 1119–1122.
- KILHAMS, B., HARTLEY, A., HUISE, M., AND DAVIS, C., 2012, Characterizing the Paleocene turbidites of the North Sea: the Mey Sandstone Member, Lista Formation, UK Central Graben: *Petroleum Geoscience*, v. 18, p. 337–354.
- LIEN, T., MIDTBØ, R.E., AND MARTINSEN, O.J., 2006, Depositional facies and reservoir quality of deep-marine sandstones in the Norwegian Sea: *Norwegian Journal of Geology*, v. 86, p. 71–92.
- LOWE, D.R., 1982, Sediment gravity flows: II. Depositional models with special reference to the deposits of high-density turbidity currents: *Journal of Sedimentary Petrology*, v. 52, p. 279–297.
- LOWE, D.R., AND GUY, M., 2000, Slurry-flow deposits in the Britannia Formation (Lower Cretaceous) North Sea: a new perspective on the turbidity currents and debris flow problem: *Sedimentology*, v. 47, p. 31–70.
- MARCHAND, A.M.E., APPS, G., LI, W., AND ROTZIEH, J.R., 2015, Depositional processes and impact on reservoir quality in deepwater Paleogene reservoirs, US Gulf of Mexico: *American Association of Petroleum Geologists, Bulletin*, v. 99, p. 1635–1648.
- MARTINSEN, O.J., LIEN, T., AND JACKSON, C., 2005, Cretaceous and Palaeogene turbidite systems in the North Sea and Norwegian Sea basins: source, staging area and basin physiography controls on reservoir development, *in* Doré, A.G., and Vining, B.A., eds., *Petroleum Geology: North-West Europe and Global Perspectives*: Geological Society of London, 6th Petroleum Geology Conference, Proceedings, p. 1147–1164.
- MARZANO, M.S., 1988, Controls on permeability for unconsolidated sands from conventional core data offshore Gulf of Mexico: *Gulf Coast Association of Geological Societies, Transactions*, v. 38, p. 113–120.
- MCBRIDE, E.F., 1989, Quartz cement in sandstones: a review: *Earth-Science Reviews*, v. 26, p. 69–112.
- MIDTBØ, R.E.A., RYKKJE, J.M., AND RAMM, M., 2000, Deep burial diagenesis and reservoir quality along the eastern flank of the Viking Graben. Evidence for illitization and quartz cementation after hydrocarbon emplacement: *Clay Minerals*, v. 35, p. 227–237.
- MORAD, S., AL-RAMADAN, K., KETZER, J.M., AND DE ROS, L.F., 2010, The impact of diagenesis on the heterogeneity of sandstone reservoirs: a review of the role of depositional facies and sequence stratigraphy: *American Association of Petroleum Geologists, Bulletin*, v. 94, p. 1267–1309.
- MORTON, A.C., WHITHAM, A.G., FANNING, C.M., AND CLAOUÉ-LONG, J., 2005, The role of East Greenland as a source of sediment to the Vøring Basin during the Late Cretaceous, *in* Wandås, B.T.G., Eide, E.A., Gradstein, F., and Nystuen, J.P., eds., *Onshore–Offshore Relationships on the North Atlantic Margin*: Norwegian Petroleum Society, Special Publication 12, p. 83–110.
- NIJOKU, C., AND PIRMEZ, C., 2011, Sedimentary controls on porosity and permeability in deepwater turbidites: *Society of Petroleum Engineers, Annual International Conference and Exhibition, Nigeria*, Conference Paper, doi:10.2118/150805-MS.
- PIRMEZ, C., BEAUBOUËF, R.T., FRIEDMANN, S.J., AND MOHRIG, D.C., 2000, Equilibrium profile and base level in submarine channels: examples from late Pleistocene systems and implications for the architecture of deepwater reservoirs, *in* Weimer, P., Slatt, R.M., Coleman, J., Rosen, N.C., Nelson, H., Bouma, A.H., Styzen, M.J., and Lawrence, D.T., eds., *Deep-Water Reservoirs of the World*: SEPM, Gulf Coast Section, 20th Annual Research Conference, p. 782–805.
- PITTMAN, E.D., AND LARESE, R.E., 1991, Compaction of lithic sands: experimental results and applications: *American Association of Petroleum Geologists, Bulletin*, v. 75, p. 1279–1299.
- PITTMAN, E.D., LARESE, R.E., AND HEALD, M.T., 1992, Clay coats: occurrence and relevance to preservation of porosity in sandstones, *in* Houseknecht, D.W., and Pittman, E.D., eds., *Origin, Diagenesis, and Petrophysics of Clay Minerals in Sandstones*: SEPM, Special Publication 47, p. 241–255.
- PRÉLAT, A., HODGSON, D.M., AND FLINT, S.S., 2009, Evolution, architecture and hierarchy of distributary deep-water deposits: a high-resolution outcrop investigation from the Permian Karoo Basin, South Africa: *Sedimentology*, v. 56, p. 2132–2154.
- PRYOR, W.A., 1973, Permeability–porosity patterns and variations in some Holocene sand bodies: *American Association of Petroleum Geologists, Bulletin*, v. 57, p. 162–189.
- RAMM, M., 2000, Reservoir quality and its relationship to facies and provenance in Middle to Upper Jurassic sequences, northeastern North Sea: *Clay Minerals*, v. 35, p. 77–94.
- ROBERTS, A.M., LUNDIN, E.R., AND KUSZNIR, N.J., 1997, Subsidence of the Vøring Basin and the influence of the Atlantic continental margin: *Geological Society of London, Journal*, v. 154, p. 551–557.
- SKOGSEID, J., AND ELDHOLM, O., 1989, Vøring Continental Margin: seismic interpretation, stratigraphy and vertical movements, *in* Eldholm, O., Thiede, J., and Taylor, E., eds., *Proceedings of the Ocean Drilling Program: Scientific Results 104*, College Station, Texas, p. 993–1030.
- SLAMA, J., WALDERHAUG, O., FONNELAND, H., KOSLER, J., AND PEDERSEN, R.B., 2011, Provenance of Neoproterozoic to Upper Cretaceous sedimentary rocks, eastern Greenland: implications for recognizing the sources of sediments in the Norwegian Sea: *Sedimentary Geology*, v. 238, p. 254–267.
- SOUTHERN, S.J., KANE, I.A., WARCHOL, M.J., PORTEN, K.W., AND MCCAFFREY, W.D., **in press**, Hybrid event beds dominated by transitional-flow facies types: character, distribution and significance in the Maastrichtian Springar Formation, north-western Vøring Basin, Norwegian Sea: *Sedimentology*.
- STALDER, P.J., 1973, Influence of crystallographic habit and aggregate structure of authigenic clay minerals on sandstone permeability: *Geologie en Mijnbouw*, v. 52, p. 217–220.
- TALLING, P.J., MASSON, D.G., SUMNER, E.J., AND MALGESINI, G., 2012, Subaqueous sediment density flows: depositional processes and deposit types: *Sedimentology*, v. 59, p. 1937–2003.
- TAYLOR, T.R., GILES, M.R., HATHON, L.A., DIGGS, T.N., BRAUNSDORF, N.R., BIRBIGLIA, G.V., KITTRIDGE, M.G., MACAULAY, C.I., AND ESPEJO, I.S., 2010, Sandstone diagenesis and reservoir quality prediction: models, myths, and reality: *American Association of Petroleum Geologists, Bulletin*, v. 94, p. 1093–1132.
- WALDERHAUG, O., 1994a, Temperatures of quartz cementation in Jurassic sandstones from the Norwegian shelf: evidence from fluid inclusions: *Journal of Sedimentary Research*, v. 64, p. 311–323.
- WALDERHAUG, O., 1994b, Precipitation rates for quartz cement in sandstones determined by fluid inclusion microthermometry and temperature history modeling: *Journal of Sedimentary Research*, v. 64, p. 324–333.
- WALDERHAUG, O., 1996, Kinetic modeling of quartz cementation and porosity loss in deeply buried sandstone reservoirs: *American Association of Petroleum Geologists, Bulletin*, v. 80, p. 731–745.
- WALDERHAUG, O., 2000, Modeling quartz cementation and porosity in Middle Jurassic Brent Group sandstones of the Kvitebjørn Field, northern North Sea: *American Association of Petroleum Geologists, Bulletin*, v. 84, p. 1325–1339.
- WALDERHAUG, O., LANDER, R.H., BJØRNUM, P.A., OELKERS, E.H., BJØRLYKKE, K., AND NADEAU, P.H., 2000, Modelling quartz cementation and porosity in reservoir sandstones: examples from the Norwegian continental shelf, *in* Worden, R., and Morad, S., eds., *Quartz Cementation in Sandstones*: International Association of Sedimentologists, Special Publication 29, p. 39–49.
- WALDERHAUG, O., ELIASSEN, A., AND AASE, N.E., 2012, Prediction of permeability in quartz-rich sandstones: examples from the Norwegian continental shelf and the Fontainebleau sandstone: *Journal of Sedimentary Research*, v. 82, p. 899–912.
- WILSON, M.D., AND STANTON, P.T., 1994, Diagenetic mechanisms of porosity and permeability reduction and enhancement, *in* Wilson, M.D., ed., *Reservoir Quality Assessment and Prediction in Clastic Rocks*: SEPM, Short Course 30, p. 59–118.